

UNCLASSIFIED

OAK RIDGE NATIONAL LABORATORY LIBRARY



3 4456 0023203 1

CBR Document No. 4
Title: THE BUILDUP OF HEAVY ISOTOPES
during thermal neutron irradiation of uranium reactor fuels
Author: J. O. Blomeke

ORNL-2126
Chemistry Cy. 4

THE BUILDUP OF HEAVY ISOTOPES

DURING THERMAL NEUTRON IRRADIATION

OF URANIUM REACTOR FUELS

J. O. Blomeke

CENTRAL RESEARCH LIBRARY
DOCUMENT COLLECTION

LIBRARY LOAN COPY

DO NOT TRANSFER TO ANOTHER PERSON

If you wish someone else to see this document,
send in name with document and the library will
arrange a loan.



**OAK RIDGE NATIONAL LABORATORY
OPERATED BY**

UNION CARBIDE NUCLEAR COMPANY

A Division of Union Carbide and Carbon Corporation

UCC

POST OFFICE BOX X • OAK RIDGE, TENNESSEE

UNCLASSIFIED

40

Printed in USA. Price _____ cents. Available from the

Office of Technical Services
U. S. Department of Commerce
Washington 25, D. C.

LEGAL NOTICE

This report was prepared as an account of Government sponsored work. Neither the United States, nor the Commission, nor any person acting on behalf of the Commission:

- A. Makes any warranty or representation, express or implied, with respect to the accuracy, completeness, or usefulness of the information contained in this report, or that the use of any information, apparatus, method, or process disclosed in this report may not infringe privately owned rights; or
- B. Assumes any liabilities with respect to the use of, or for damages resulting from the use of any information, apparatus, method, or process disclosed in this report.

As used in the above, "person acting on behalf of the Commission" includes any employee or contractor of the Commission to the extent that such employee or contractor prepares, handles or distributes, or provides access to, any information pursuant to his employment or contract with the Commission.

ORNL-2126

Contract No. W-7405-eng-26

CHEMICAL TECHNOLOGY DIVISION

PROCESS DESIGN SECTION

THE BUILDUP OF HEAVY ISOTOPES DURING THERMAL NEUTRON
IRRADIATION OF URANIUM REACTOR FUELS

J. O. Blomeke

Date Issued

DEC 26 1956

OAK RIDGE NATIONAL LABORATORY
Operated by
UNION CARBIDE NUCLEAR COMPANY
A Division of Union Carbide and Carbon Corporation
Post Office Box X
Oak Ridge, Tennessee



3 4456 0023203 1

UNCLASSIFIED

-ii-

ORNL-2126
Chemistry
TID-4500 (12th ed.)

INTERNAL DISTRIBUTION

1. C. E. Center
2. Biology Library
3. Health Physics Library
4. Central Research Library
5. Reactor Experimental
Engineering Library
7-26. Laboratory Records Department
27. Laboratory Records, ORNL R.C.
28. A. M. Weinberg
29. L. B. Emlet (K-25)
30. J. P. Murray (Y-12)
31. J. A. Swartout
32. E. H. Taylor
33. E. D. Shipley
34-35. F. L. Culler
36. M. L. Nelson
37. W. H. Jordan
38. C. P. Keim
39. J. H. Frye, Jr.
40. S. C. Lind
41. A. H. Snell
42. A. Hollaender
43. K. Z. Morgan
44. M. T. Kelley
45. T. A. Lincoln
46. R. S. Livingston
47. A. S. Householder
48. C. S. Harrill
49. C. E. Winters
50. D. W. Cardwell
51. E. M. King
52. W. K. Eister
53. F. R. Bruce
54. D. E. Ferguson
55. R. B. Lindauer
56. H. E. Goeller
57. D. D. Cowen
58. R. A. Charpie
59. J. A. Lane
60. M. J. Skinner
61. R. E. Blanco
62. G. E. Boyd
63. W. E. Unger
64. R. R. Dickison
65. A. T. Gresky
66. E. D. Arnold
67. C. E. Guthrie
68. J. W. Ullmann
69. K. B. Brown
70. K. O. Johnsson
71. H. M. McLeod
72. J. C. Bresee
73. J. Halperin
74-79. J. O. Blomeke
80. R. W. Stoughton
81. E. J. Frederick
82. H. E. Williamson
83. J. T. Roberts
84. R. A. Dandl
85. E. G. Struxness
86. S. Peterson
87. W. W. Weinrich (consultant)
88. M. D. Peterson (consultant)
89. D. L. Katz (consultant)
90. G. T. Seaborg (consultant)
91. M. Benedict (consultant)
92. C. E. Larson (consultant)
93. ORNL - Y-12 Technical Library,
Document Reference Section

EXTERNAL DISTRIBUTION

94. R. F. Bacher, California Institute of Technology
95. Division of Research and Development, AEC, ORO
96-680. Given distribution as shown in TID-4500 under Chemistry category
(200 copies - OTS)

UNCLASSIFIED

CONTENTS

	<u>Page</u>
1.0 Abstract -----	1
2.0 Introduction -----	1
3.0 Cross-Sections -----	2
Fig. 1 Schematic showing heavy isotope buildup from U^{233} -----	3
Fig. 2 Schematic showing heavy isotope buildup from U^{234} -----	4
Fig. 3 Schematic showing heavy isotope buildup from U^{235} -----	5
Fig. 4 Schematic showing heavy isotope buildup from U^{236} -----	6
Fig. 5 Schematic showing heavy isotope buildup from U^{238} -----	7
Fig. 6 Burnup of primary isotopes as a function of the product of thermal neutron flux and irradiation time -----	8
4.0 References -----	9
5.0 Appendix: Calculations -----	11
Fig. 1 Schematic showing heavy isotope buildup from U^{233} -----	16
Fig. 1-A Buildup of U^{234} , U^{235} , and U^{236} from U^{233} as a function of the product of irradiation time and thermal neutron flux -----	17
Fig. 1-B Buildup of U^{237} from U^{233} -----	18
Fig. 1-C Buildup of Np^{237} from U^{233} -----	19
Fig. 1-D Buildup of Np^{238} from U^{233} -----	20
Fig. 1-E Buildup of Pu^{238} from U^{233} -----	21
Fig. 2 Schematic showing heavy isotope buildup from U^{234} -----	22
Fig. 2-A Buildup of U^{235} and U^{236} from U^{234} as a function of the product of irradiation time and thermal neutron flux -----	23
Fig. 2-B Buildup of U^{237} from U^{234} -----	24
Fig. 2-C Buildup of Np^{237} from U^{234} -----	25
Fig. 2-D Buildup of Np^{238} from U^{234} -----	26
Fig. 2-E Buildup of Pu^{238} from U^{234} -----	27
Fig. 3 Schematic showing heavy isotope buildup from U^{235} -----	28
Fig. 3-A Buildup of U^{236} from U^{235} as a function of the product of irradiation time and thermal neutron flux -----	29
Fig. 3-B Buildup of U^{237} from U^{235} -----	30
Fig. 3-C Buildup of Np^{237} from U^{235} -----	31
Fig. 3-D Buildup of Np^{238} from U^{235} -----	32
Fig. 3-E Buildup of Pu^{238} from U^{235} -----	33
Fig. 3-F Buildup of Pu^{239} from U^{235} -----	34
Fig. 4 Schematic showing heavy isotope buildup from U^{236} -----	35
Fig. 4-A Buildup of U^{237} from U^{236} -----	36
Fig. 4-B Buildup of Np^{237} from U^{236} -----	37

	<u>Page</u>
Fig. 4-C Buildup of Np ²³⁸ from U ²³⁶ -----	38
Fig. 4-D Buildup of Pu ²³⁸ from U ²³⁶ -----	39
Fig. 4-E Buildup of Pu ²³⁹ from U ²³⁶ -----	40
Fig. 4-F Buildup of Pu ²⁴⁰ from U ²³⁶ -----	41
Fig. 4-G Buildup of Pu ²⁴¹ from U ²³⁶ -----	42
Fig. 4-H Buildup of Pu ²⁴² from U ²³⁶ -----	43
Fig. 5 Schematic showing heavy isotope buildup from U ²³⁸ -----	44
Fig. 5-A Buildup of U ²³⁷ from U ²³⁸ -----	45
Fig. 5-B Buildup of Np ²³⁷ from U ²³⁸ -----	46
Fig. 5-C Buildup of Np ²³⁸ from U ²³⁸ -----	47
Fig. 5-D Buildup of Pu ²³⁸ from U ²³⁸ -----	48
Fig. 5-E Buildup of Np ²³⁹ from U ²³⁸ -----	49
Fig. 5-F Buildup of Pu ²³⁹ from U ²³⁸ -----	50
Fig. 5-G Buildup of Pu ²⁴⁰ from U ²³⁸ -----	51
Fig. 5-H Buildup of Pu ²⁴¹ from U ²³⁸ -----	52
Fig. 5-I Buildup of Pu ²⁴² from U ²³⁸ -----	53
Fig. 5-J Buildup of Am ²⁴¹ from U ²³⁸ -----	54
Fig. 5-K Buildup of Am ²⁴² from U ²³⁸ -----	55
Fig. 5-L Buildup of Am ²⁴³ from U ²³⁸ -----	56
Fig. 5-M Buildup of Cm ²⁴² from U ²³⁸ -----	57
Fig. 5-N Buildup of Cm ²⁴⁴ from U ²³⁸ -----	58

1.0 ABSTRACT

Curves suitable for predicting the buildup of heavy isotopes in uranium reactor fuel of any likely initial isotopic composition are presented. The curves were computed for seven values of thermal neutron flux between 10^{12} and $10^{15} \text{ n/cm}^2/\text{sec}$, assuming constant flux, and extended to flux-times of $3 \times 10^{21} \text{ n/cm}^2$.

2.0 INTRODUCTION

Neutron irradiation of uranium results in formation of a number of uranium and transuranic isotopes, some of which have nuclear properties that render them undesirable as reactor fuel constituents. The effect of these isotopes on reactivity, based on single, long-term irradiation of fuel of various enrichments, has been considered by many investigators.¹⁻⁵ Ullmann⁶ and Arnold⁷ investigated the buildup of U^{236} , U^{237} , Np^{237} , and Pu^{238} in recycled U^{235} fuels and showed how, even with partial removal of U^{236} in each cycle, these products could grow to such levels as to influence the type and frequency of chemical processing and fuel fabrication.

The present calculations, performed on an analog computer, have been carried out primarily to serve as a tool in studying transuranic activities of interest to the chemical processer. They permit rapid estimation of heavy-element concentration in irradiated fuels of any likely initial composition, and are, consequently, especially suitable for studying the buildup in fuel recycled through chemical processing, fabrication, and irradiation a number of times. Results are presented in the form of curves expressing the growth of individual isotopes from pure U^{233} , U^{234} , U^{235} , U^{236} , and U^{238} during irradiation at constant flux. Seven values of thermal neutron flux between 10^{12} and $10^{15} \text{ n/cm}^2/\text{sec}$ were considered, and irradiations were extended to flux-times near $3 \times 10^{21} \text{ n/cm}^2$.

The author gratefully acknowledges the assistance and suggestions received

from R. A. Dandl relating to the use of the analog computer for these calculations. In addition, he would like to express his appreciation to J. Halperin and R. W. Stoughton for their many enlightening discussions on heavy element cross-sections and to H. E. Williamson for his help in operation of the computer.

3.0 CROSS-SECTIONS

The paths for buildup of the significant transuranic isotopes from the five long-lived uranium isotopes are given in Figs. 1 through 5. The mechanism of production is primarily that of n,γ reactions and β decay, but also considered here are the $n,2n$ reaction of U^{238} and the partial decay of metastable Am^{242} by electron capture (Fig. 5). In addition, destruction of certain isotopes by fission and α decay was taken into account.

The choice of the best cross-section values for use in the present calculations was complicated in many cases by uncertainties attributable to resonance absorption. Those isotopes known or suspected to possess large resonance integrals must be assigned effective reactor cross-sections for computation of reaction rates. The effective reactor cross-sections quoted here are intended to be used with thermal fluxes determined from a cadmium ratio measurement and the 2200 m/sec cross-section of a $1/v$ detector. However, in those cases where epithermal absorption is sizable, the precise value of the effective cross-section to be used is so dependent on the particular reactor, position in the lattice, and operating peculiarities that the choice of an exact value for such calculations cannot be taken too seriously. The values selected are a representative set approximating those for the MTR configuration;^a consequently, the buildup of isotopes reported here must be interpreted in the light of this approximation.

^a The MTR is a thermal reactor operated with highly enriched U^{235} fuel, present in the form of thin plates of aluminum-uranium alloy. It is cooled by forced convection of natural water over the fuel plates.

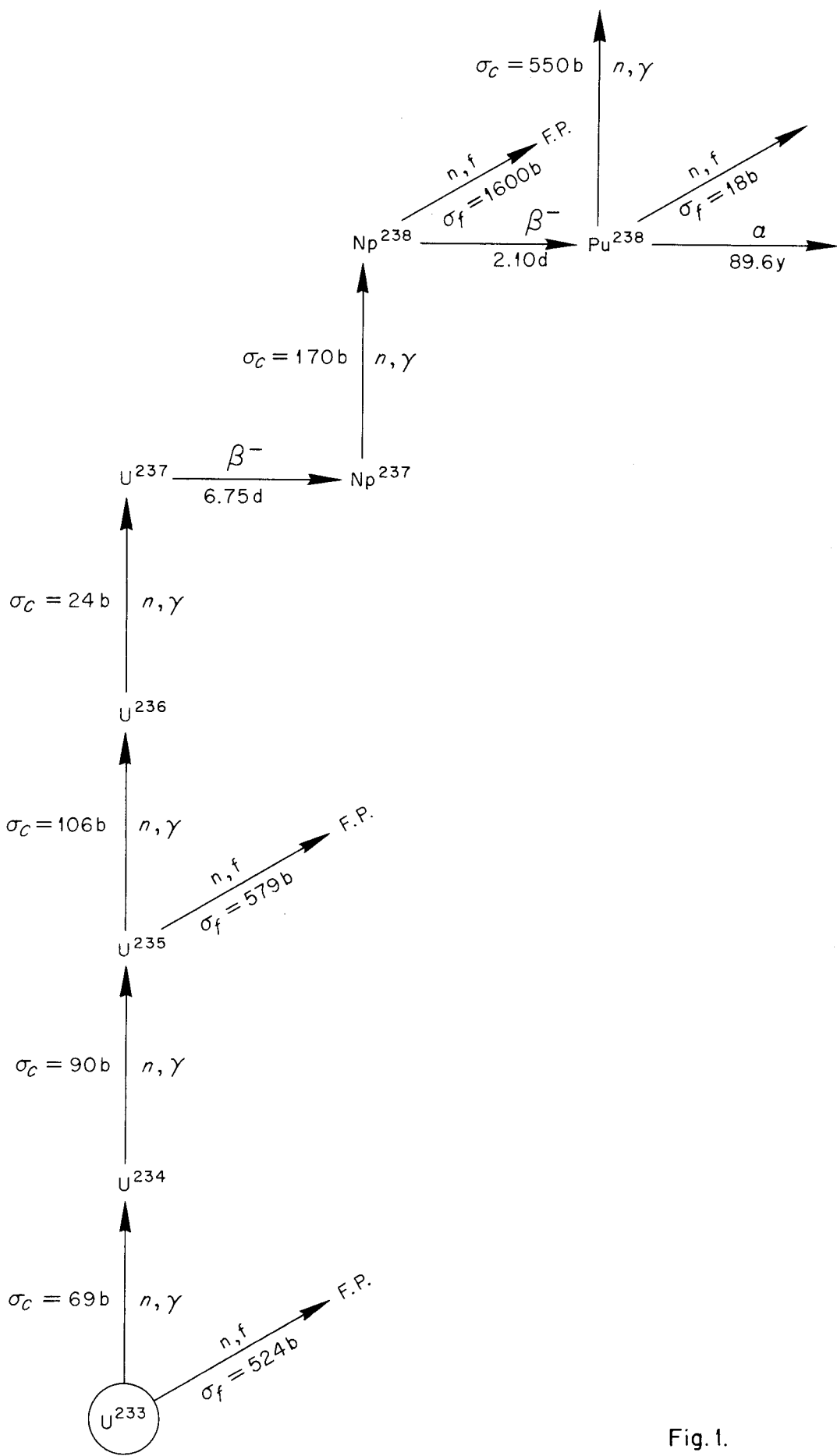


Fig. 1.

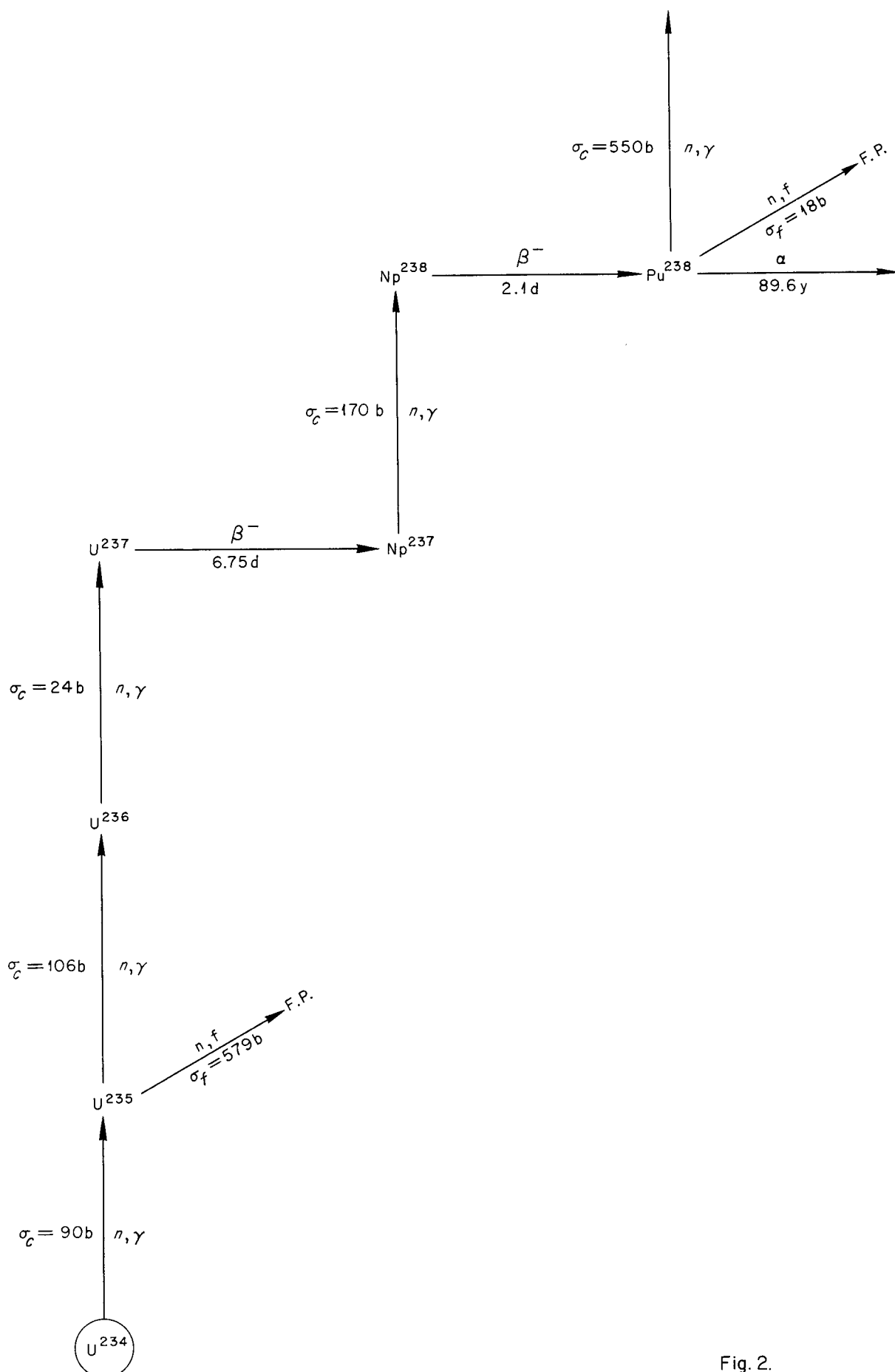


Fig. 2.

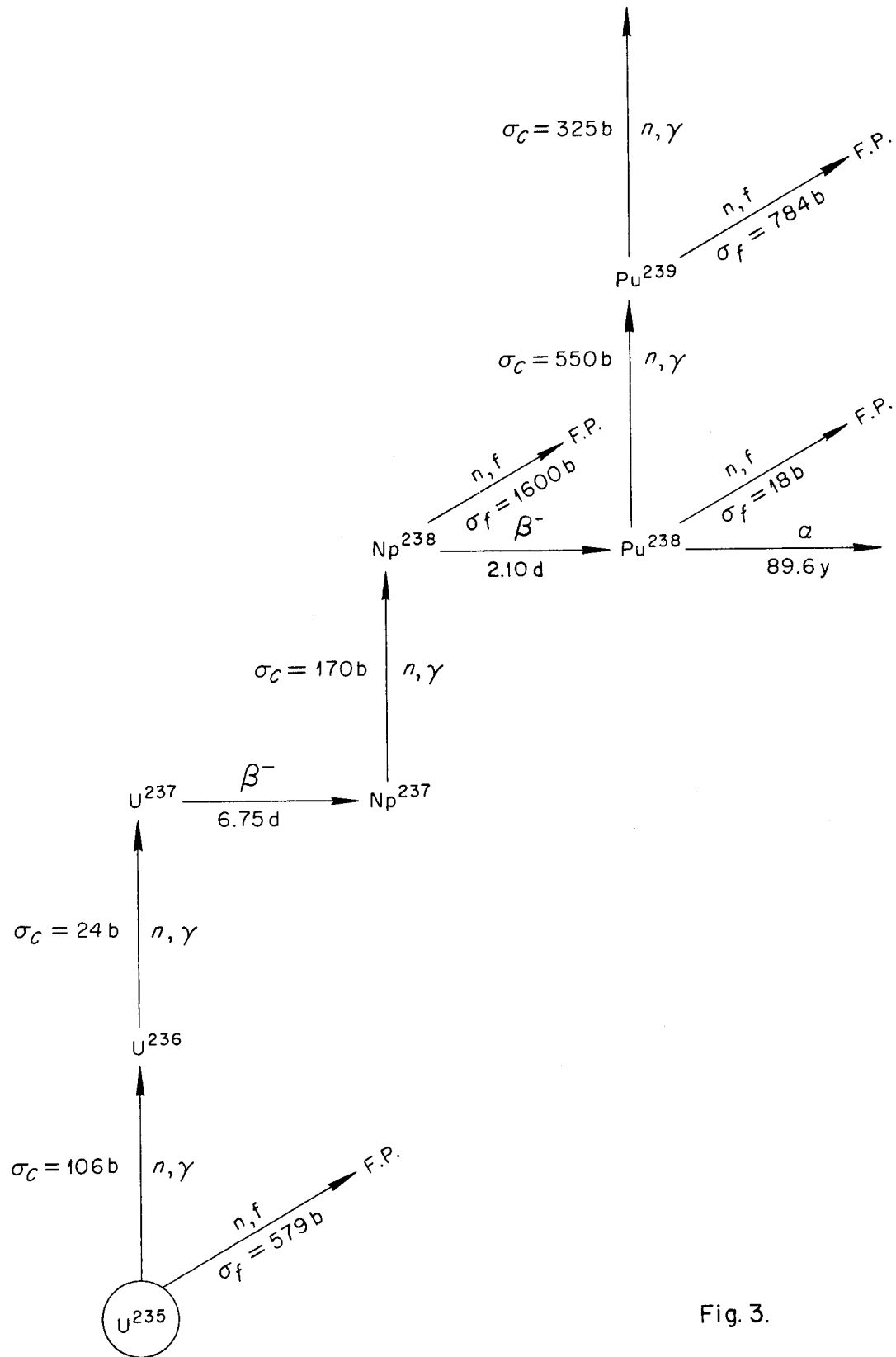


Fig. 3.

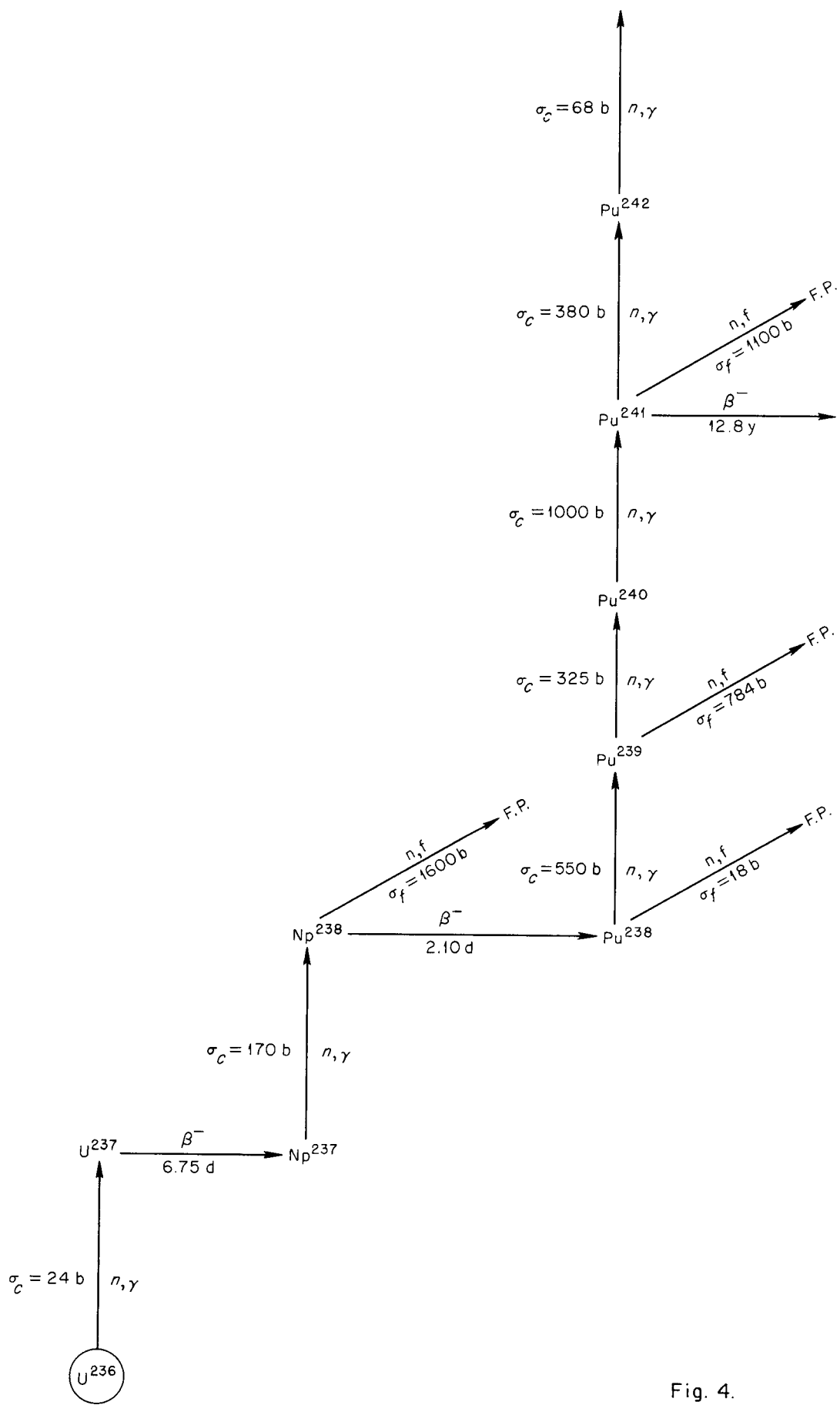


Fig. 4.

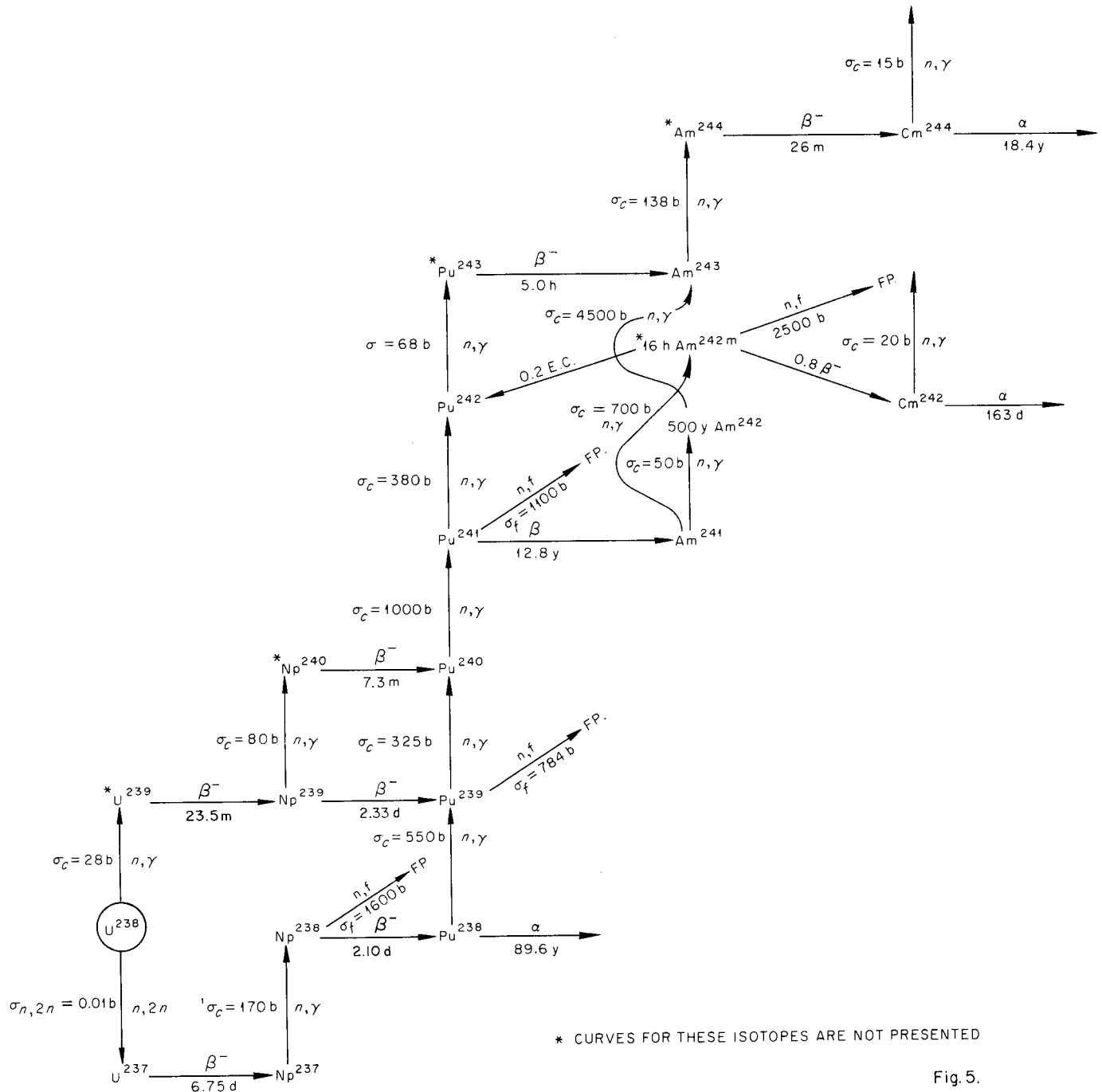


Fig. 5.

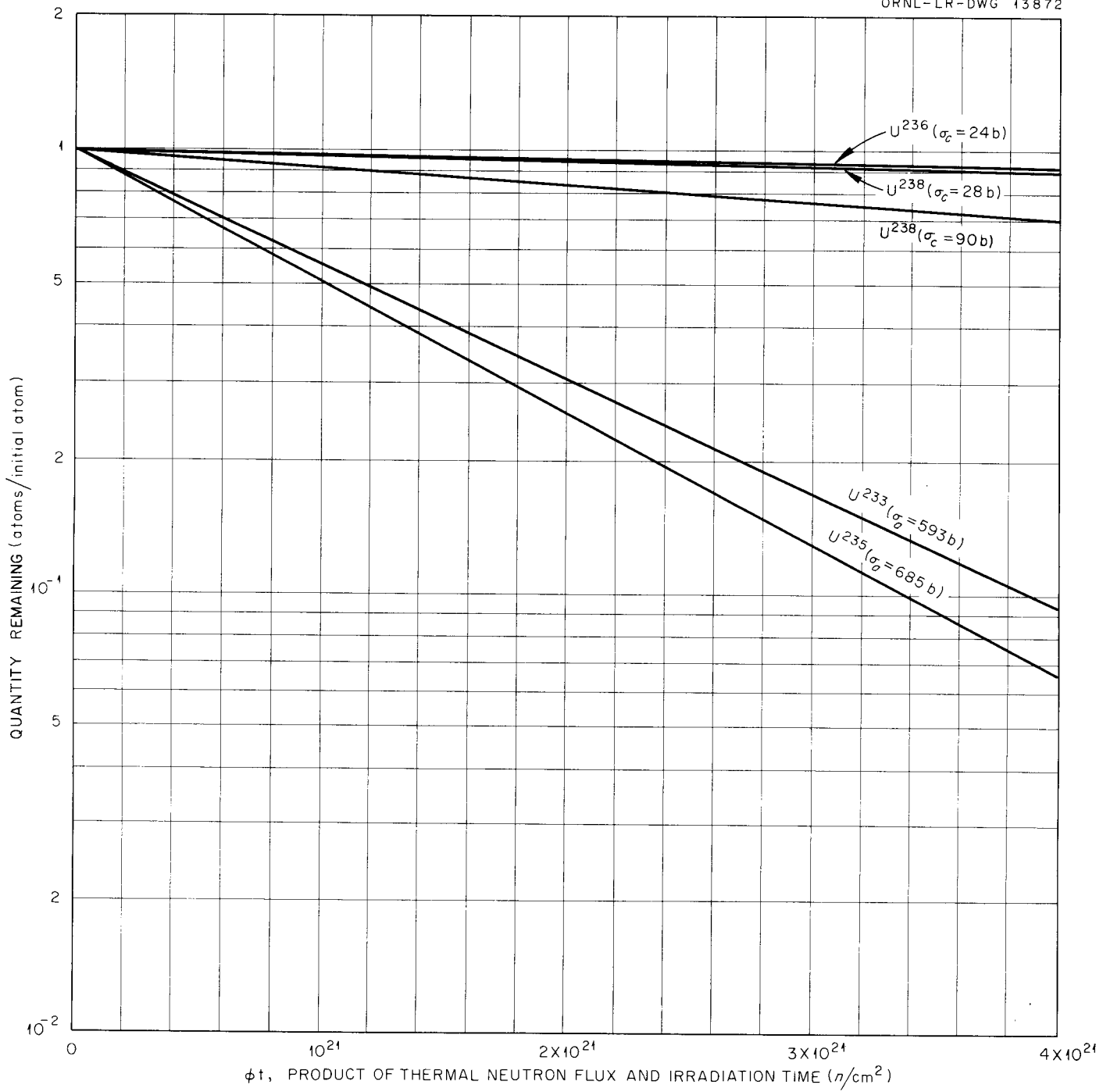


Fig. 6. Burnup of Primary Isotopes as a Function of the Product of Thermal Neutron Flux and Irradiation Time.

The majority of the cross-section values were taken from the compilation of Hughes and Harvey.⁸ The exceptions were as follows:

U^{233} , U^{235} , and Pu^{239} : The so-called international values proposed at the Geneva Nuclear Energy Conference, August 1955, and reported in Nucleonics⁹ were used. The U^{235} and Pu^{239} values were corrected for their non- $1/v$ character by use of the factors given by Harvey and Hughes.

U^{234} : An apparent inconsistency exists between the 2200-m/sec absorption cross-section of 92 ± 7 barns and the reactor activation cross-section of 72 ± 10 barns reported by Harvey and Hughes. In view of the large resonance absorption expected, it was felt that a choice of 90 barns, near the higher value, was justified.

U^{236} : Resonance absorption by this isotope is known to be large, and in dilute concentrations this can be expected to result in a reactor cross-section considerably in excess of the 2200-m/sec value. Consequently, the value of 24 barns reported by Auclair et al.¹⁰ was chosen for these calculations.

U^{238} : An estimated value of 28 barns was used in these calculations, based on the 280-barn resonance integral of U^{238} .

In slightly enriched systems where the effective reactor cross-section would be appreciably less, the levels of the respective daughters in the U^{238} chain can be found with only slight error by multiplying the presently calculated values by the ratio of the appropriate cross-section to 28 barns.

U^{238} : An n-2n cross-section of 10 millibarns was estimated for use in this work.

Pu^{238} : The value of 552 barns reported by Butler, Lounsbury, and Merritt¹¹ was adopted.

Pu^{240} : An estimated value of 1000 barns was used, based on the thermal cross-section of about 500 barns and the large resonance at 1 ev.

Pu^{242} : The value of 68 barns reported by Butler, Lounsbury, and Merritt¹¹ was used.

Am^{243} : A value of 138 barns was used, based on work reported by Butler, Lounsbury, and Merritt.¹¹

4.0 REFERENCES

1. J. R. Triplett, "Reactivity Changes in Isotope Yields at High Exposures," HW-33912 (January 20, 1955).
2. E. R. Cohen et al., "Long-Term Irradiation of Nuclear Fuels," TID-10066 (September 15, 1954).

3. J. C. Carter and J. M. West, "Reactivity as a Function of Irradiation Time in Thermal Reactors," TID-10008 (Dec. 15, 1953).
4. W. R. Clancey, "Variation Throughout Reactor Lifetime of the Regeneration Factor, η , for Slightly Enriched Uranium," WAPD-93 (Dec. 1953).
5. E. F. Weisner, "Low Enrichment Thermal Uranium Reactors for the Production of Plutonium and Useful Power," NAA-SR-179 (July 7, 1952).
6. J. W. Ullmann, ORNL, unpublished work (1954).
7. E. D. Arnold, "Effect of Recycle of Uranium Through Reactor and Gaseous Diffusion Plant on Buildup of Important Transmutation Products in Irradiated Power Reactor Fuels," ORNL-2104 (August 21, 1956).
8. D. J. Hughes and J. A. Harvey, "Neutron Cross-Sections," BNL-325 (July 1, 1955).
9. Nucleonics, 13 (No. 9): 16 (1955).
10. J. M. Auclair, P. Hubert, R. Joly, and G. Vendryes, "Mesure de la efficace de capture de U²³⁶ pour un spectre de neutrons de pile," Comp. rend. 241: 392-393 (1955).
11. J. P. Butler, M. Lounsbury, and J. Merritt, "Preparation and Properties of Pu²⁴²," paper presented at Symposium on Nuclear and Radiochemistry, McGill University, Montreal, Canada (Sept. 7-9, 1955).

APPENDIX

5.0 CALCULATIONS

Differential equations were set up expressing the rates of production and destruction of each isotope along the paths indicated in Figs. 1 through 5. As an illustration, the set of simultaneous equations representing the U²³⁵ chain given in Fig. 3 will be presented. In the equations, σ_a denotes the total, or absorption cross-section; σ_c equals the capture cross-section for n,γ reactions; σ_f = fission cross-section; λ is the decay constant = ln 2/half-life; N = the number of atoms present at irradiation time t; N^0 = the number of atoms initially present at zero irradiation time; ϕ = thermal neutron flux. The conventional method of denoting isotopes by use of the last digit of the atomic number and the last digit of the isotopic mass is employed throughout this report.

$$\text{For } U^{235}: \frac{dN_{25}}{dt} = -(\sigma_a)_{25} \phi N_{25}^0$$

$$U^{236}: \frac{dN_{26}}{dt} = (\sigma_c)_{25} \phi N_{25} - (\sigma_c)_{26} \phi N_{26}$$

$$U^{237}: \frac{dN_{27}}{dt} = (\sigma_c)_{26} \phi N_{26} - \lambda_{27} N_{27}$$

$$Np^{237}: \frac{dN_{37}}{dt} = \lambda_{27} N_{27} - (\sigma_c)_{37} \phi N_{37}$$

$$Np^{238}: \frac{dN_{38}}{dt} = (\sigma_c)_{37} \phi N_{37} - (\sigma_f)_{38} \phi N_{38} - \lambda_{38} N_{38}$$

$$Pu^{238}: \frac{dN_{48}}{dt} = \lambda_{38} N_{38} - (\sigma_a)_{48} \phi N_{48} - \lambda_{48} N_{48}$$

$$Pu^{239}: \frac{dN_{49}}{dt} = (\sigma_c)_{48} \phi N_{48} - (\sigma_a)_{49} \phi N_{49}$$

These equations were simulated on an Electronics Associates Group 16-31R linear analog computer and solved, maintaining ϕ constant. Results in the form

of curves expressing the buildup of individual isotopes as a function of irradiation time were obtained with Brown Electronik recorders for values of $\phi = 10^{12}, 3 \times 10^{12}, 10^{13}, 3 \times 10^{13}, 10^{14}, 3 \times 10^{14}$, and $10^{15} \text{ n/cm}^2/\text{sec}$. These curves were reproduced as tracings for this report and were scaled along both coordinates in order to yield the maximum sensitivity for reading and interpolation. It is believed that their precision is in all cases within 10 percent of the exact solutions of the equations. This is less than the uncertainties associated with most of the cross-section values used in the calculations. The use of the curves can best be explained by recourse to an example.

Example. What is the amount and isotopic composition of plutonium produced in a fuel assembly after irradiation at average thermal neutron flux of $3 \times 10^{14} \text{ n/cm}^2/\text{sec}$ for 34.7 days ($t = 3 \times 10^6 \text{ sec}$)? It is assumed that the assembly contains, initially, 100 g of U^{235} , 7 g of U^{236} , 6 g of U^{238} , and 1 g of U^{234} .

Solution. By reference to Fig. 6, it can be seen that the irradiation of this assembly equivalent to a flux-time of $9 \times 10^{20} \text{ n/cm}^2$ corresponds to a U^{235} burnup of $(1-0.54)100 = 46$ percent. The numbers of atoms of each uranium isotope initially present are:

$$N_{24}^o = \frac{(1)(6.02 \times 10^{23})}{(234)} = 2.57 \times 10^{21} \text{ atoms}$$

$$N_{25}^o = \frac{(100)(6.02 \times 10^{23})}{(235)} = 2.57 \times 10^{23} \text{ atoms}$$

$$N_{26}^o = \frac{(7)(6.02 \times 10^{23})}{(236)} = 1.80 \times 10^{22} \text{ atoms}$$

$$N_{28}^o = \frac{(6)(6.02 \times 10^{23})}{(238)} = 1.54 \times 10^{22} \text{ atoms}$$

Inspection of Figs. 2 through 5 indicates that plutonium isotopes will be formed along four primary paths: by n,γ reactions with U^{238} , $n,2n$ reactions

with U^{238} , and n, γ reactions with U^{235} and U^{236} . The contribution from U^{234} will be inconsequential because of its low initial concentration and longer path. For the case of plutonium buildup from U^{235} , only two isotopes need be considered, Pu^{238} and Pu^{239} . Using Fig. 3-F, the time factor, F , for a flux of 3×10^{14} is seen to be 10^5 , and the concentration factor, $f = 1.9 \times 10^3$. From the time factor, the scaled irradiation time, τ , is calculated as

$$\tau = t/F = 3 \times 10^6 / 10^5 = 30 \text{ sec}$$

From the curve for $\phi = 3 \times 10^{14}$, it is seen that a concentration ratio, n_{28} , of 0.027 corresponds to $\tau = 30$. Using the concentration factor, $f = 1.9 \times 10^3$, it is seen that

$$N_{48}/N_{25}^0 = n_{48}/f = 0.027/1.9 \times 10^3 = 1.42 \times 10^{-5} \text{ atom of } Pu^{238} \text{ per initial atom of } U^{235}$$

The total atoms of Pu^{238} produced from U^{235} in the fuel assembly is

$$N_{48} = (1.42 \times 10^{-5}) (2.57 \times 10^{23}) = 3.6 \times 10^{18} \text{ atoms}$$

The amount of Pu^{239} produced from U^{235} can be computed in a similar fashion, using Fig. 3-F. At $\tau = 30$, n_{49} is equal to 0.008. Therefore, noting that $f = 7 \times 10^3$, $N_{49}/N_{25}^0 = N_{49}/f = 0.008/7 \times 10^3 = 1.14 \times 10^{-6}$ atom Pu^{239} /initial atom U^{235} . Total atoms Pu^{239} from U^{235} , $N_{49} = (1.14 \times 10^{-6}) (2.57 \times 10^{23}) = 2.9 \times 10^{17}$ atoms.

The production of plutonium isotopes from U^{236} and U^{238} is calculated from the appropriate curves in the same manner as was done for U^{235} . The results are summarized in Tables 1 and 2. To obtain the total amounts of each isotope present at reactor shutdown, the contributions from U^{235} , U^{236} , and U^{238} are added, yielding

$$\text{Total } Pu^{238} = 3.6 \times 10^{18} + 1.06 \times 10^{19} + 4.2 \times 10^{15} = 1.42 \times 10^{19} \text{ atoms}$$

$$\text{Total Pu}^{239} = 2.9 \times 10^{17} + 9.4 \times 10^{17} + 2.2 \times 10^{19} = 2.3 \times 10^{19} \text{ atoms}$$

$$\text{Total Pu}^{240} = 5 \times 10^{16} + 2.8 \times 10^{19} = 2.8 \times 10^{19} \text{ atoms}$$

$$\text{Total Pu}^{241} = 7 \times 10^{15} + 6.5 \times 10^{18} = 6.5 \times 10^{18} \text{ atoms}$$

$$\text{Total Pu}^{242} = 6.2 \times 10^{17} \text{ atoms}$$

Table 1. Production of Plutonium from U²³⁶

$t = 3 \times 10^6$ sec; $\phi = 3 \times 10^{14}$ n/cm²/sec
Time Factor, $F = 10^5$; $\tau = t/F = 30$

Isotope, <i>i</i>	Fig. No.	<i>n_i</i>	Concen. Factor, <i>f</i>	N_i/N_{26}^0 = N_i/f	$N_i =$ $(N_i/N_{26}^0)(1.8 \times 10^{22})$
Pu ²³⁸	4-D	0.083	1.4×10^2	5.9×10^{-4}	1.06×10^{19}
Pu ²³⁹	4-E	0.026	5×10^2	5.2×10^{-5}	9.4×10^{17}
Pu ²⁴⁰	4-F	0.009	3×10^3	3×10^{-6}	5×10^{16}
Pu ²⁴¹	4-G	0.003	8×10^3	4×10^{-7}	7×10^{15}
Pu ²⁴²	4-H	-	-	-	-

Table 2. Production of Plutonium from U²³⁸

$t = 3 \times 10^6$ sec; $\phi = 3 \times 10^{14}$ n/cm²/sec
Time Factor, $F = 105$; $\tau = t/F = 30$

Isotope, <i>i</i>	Fig. No.	<i>n_i</i>	Concen. Factor, <i>f</i>	N_i/N_{28}^0 = N_i/f	$N_i =$ $(N_i/N_{28}^0)(1.54 \times 10^{22})$
Pu ²³⁸	5-D	0.082	3×10^5	2.7×10^{-7}	4.2×10^{15}
Pu ²³⁹	5-F	0.57	40	1.43×10^{-3}	2.2×10^{19}
Pu ²⁴⁰	5-G	0.27	1.5×10^2	1.80×10^{-3}	2.8×10^{19}
Pu ²⁴¹	5-H	0.083	2×10^2	4.2×10^{-4}	6.5×10^{18}
Pu ²⁴²	5-I	0.024	6×10^2	4.0×10^{-5}	6.2×10^{17}

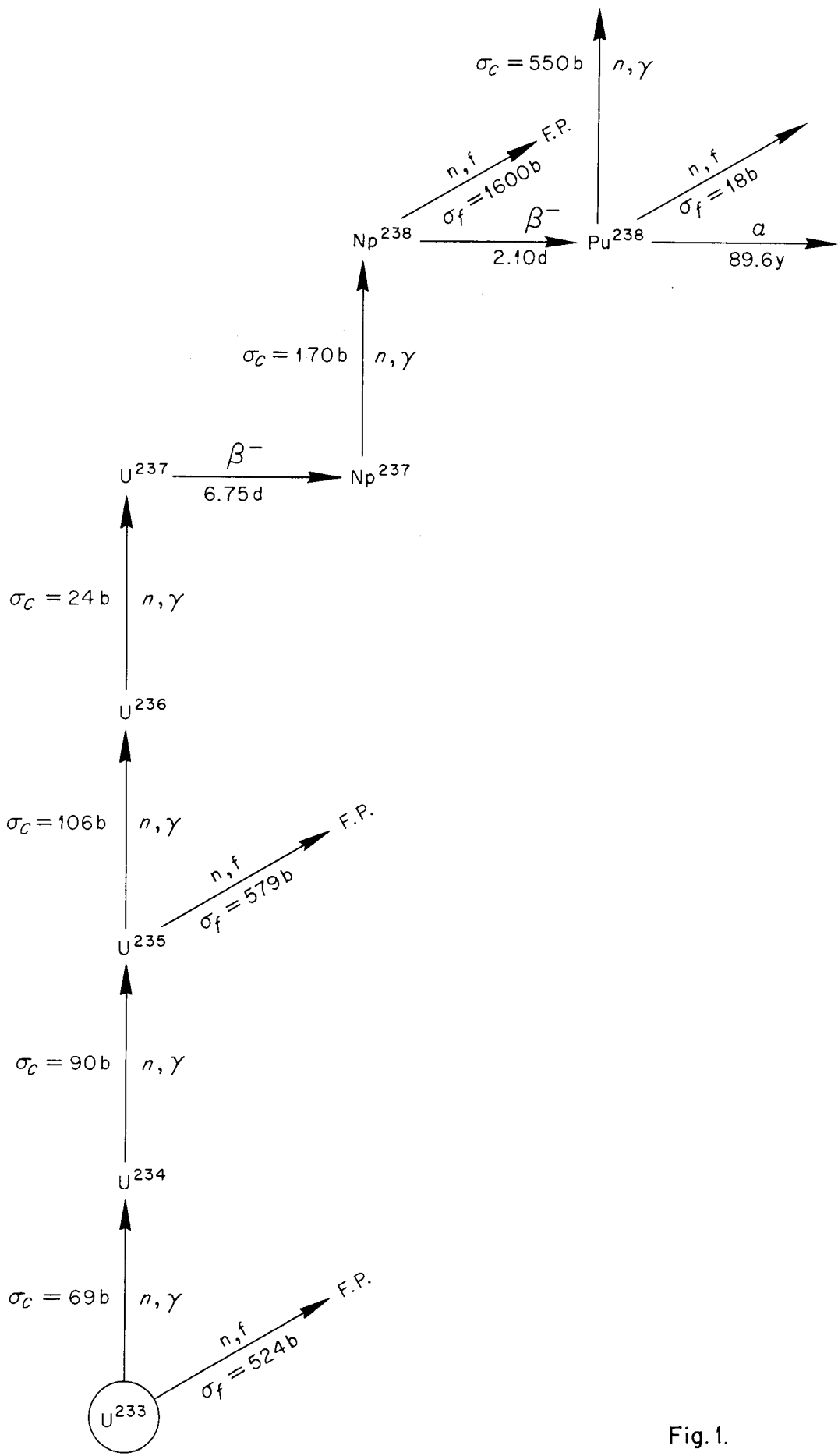


Fig. 1.

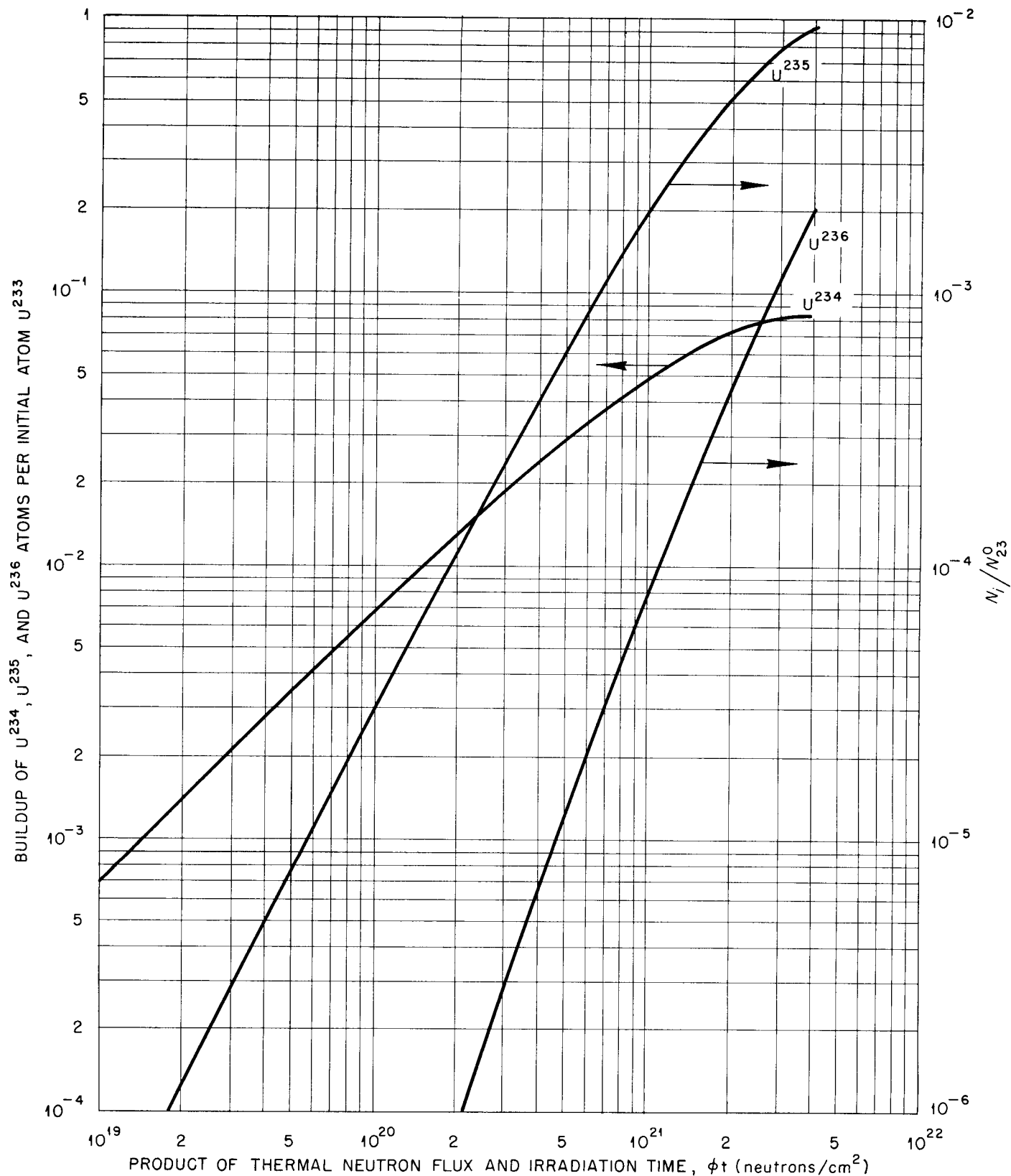
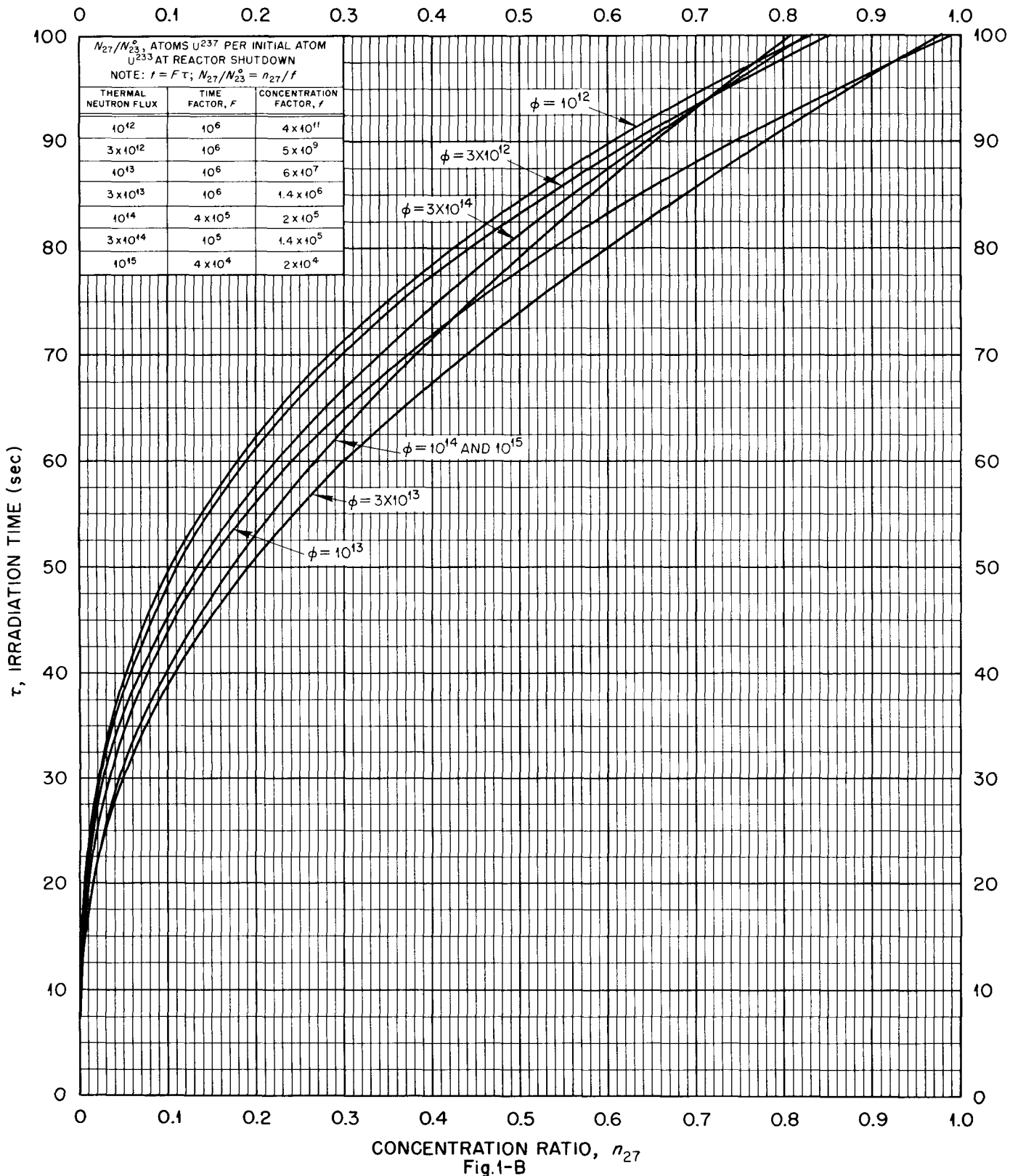


Fig. I-A. Buildup of U^{234} , U^{235} and U^{236} from U^{233} as a Function of the Product of Irradiation Time and Thermal Neutron Flux.



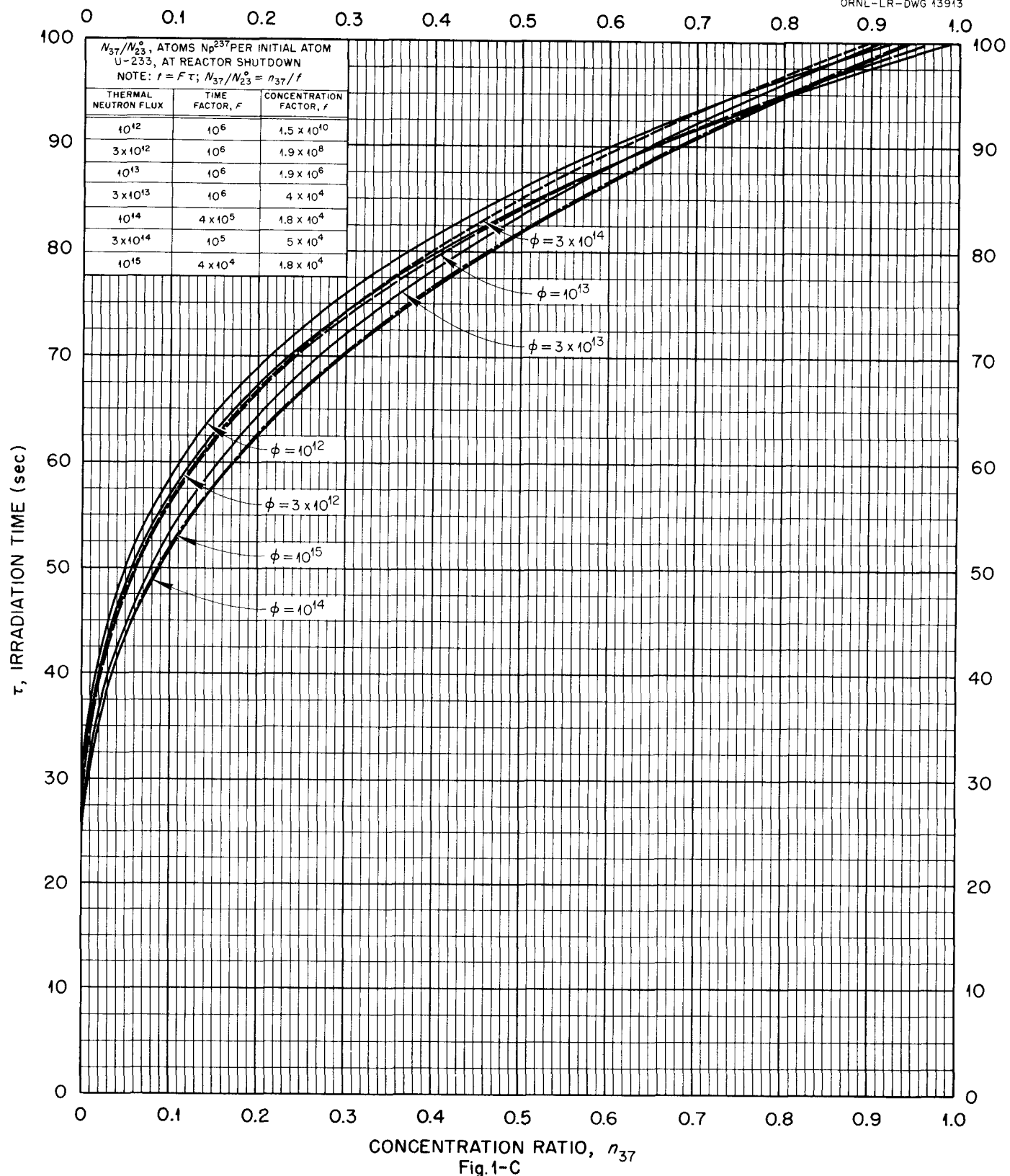
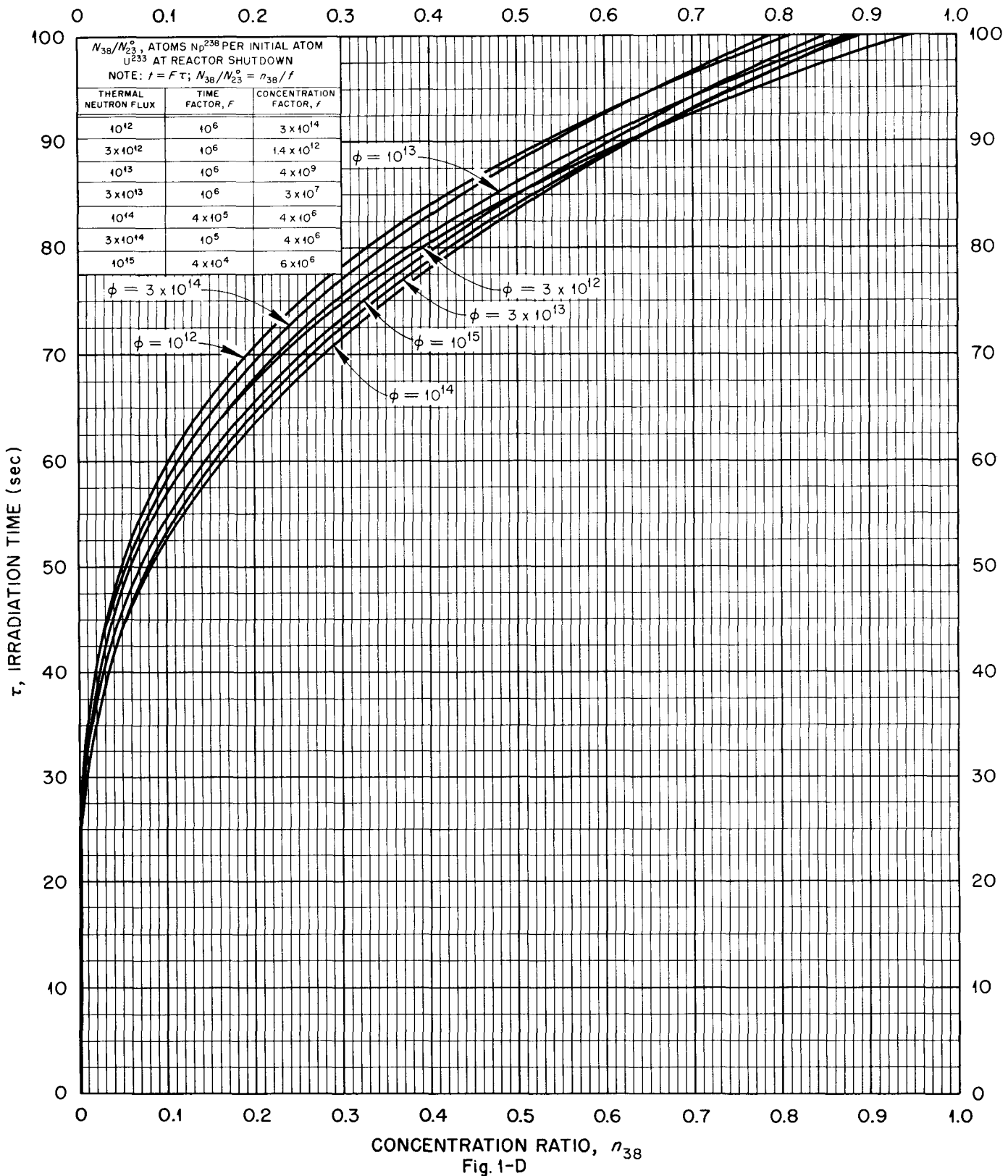


Fig.1-C



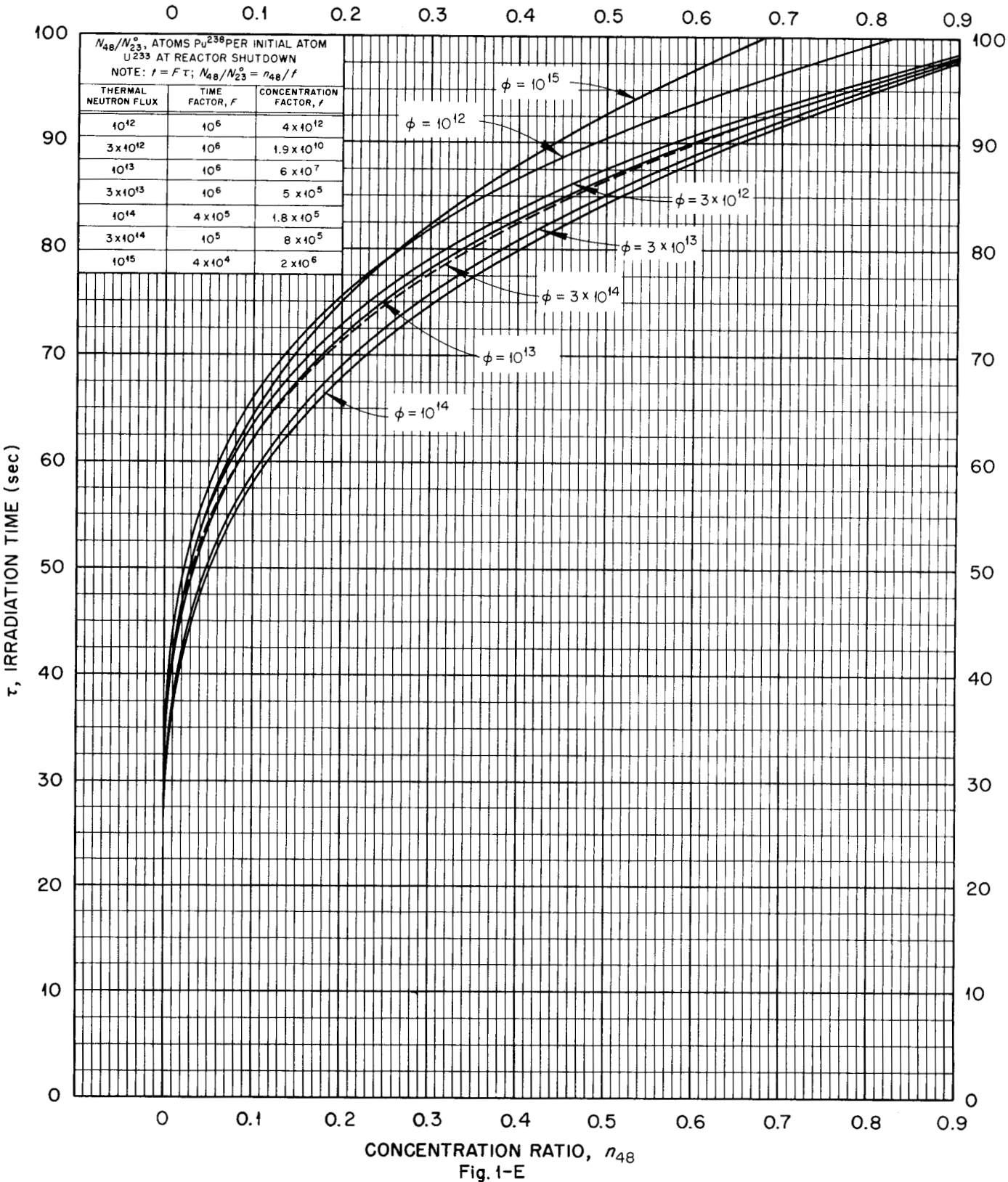
CONCENTRATION RATIO, n_{48}

Fig. 1-E

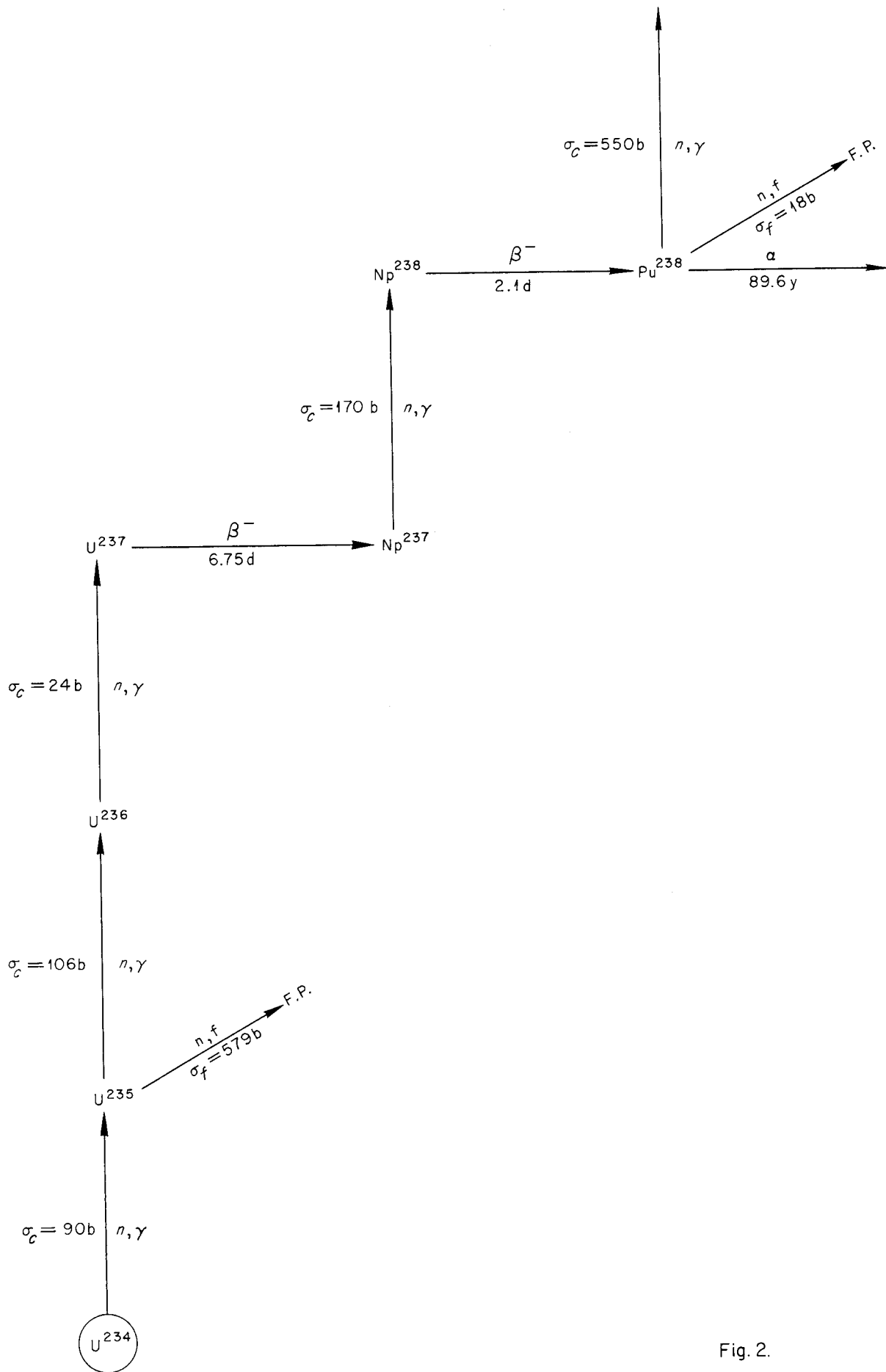


Fig. 2.

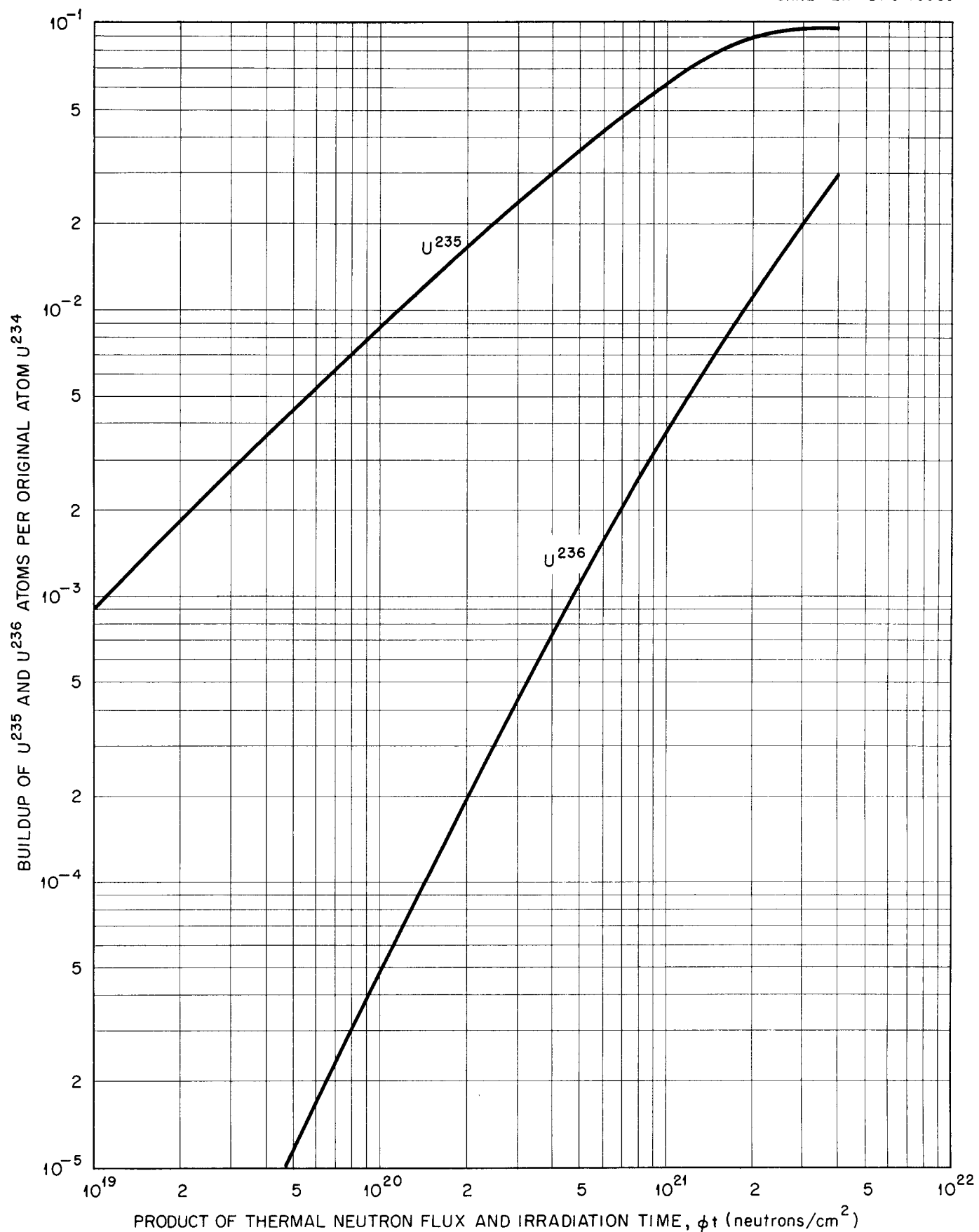


Fig. 2-A. Buildup of U^{235} and U^{236} from U^{234} as a Function of the Product of Irradiation Time and Thermal Neutron Flux.

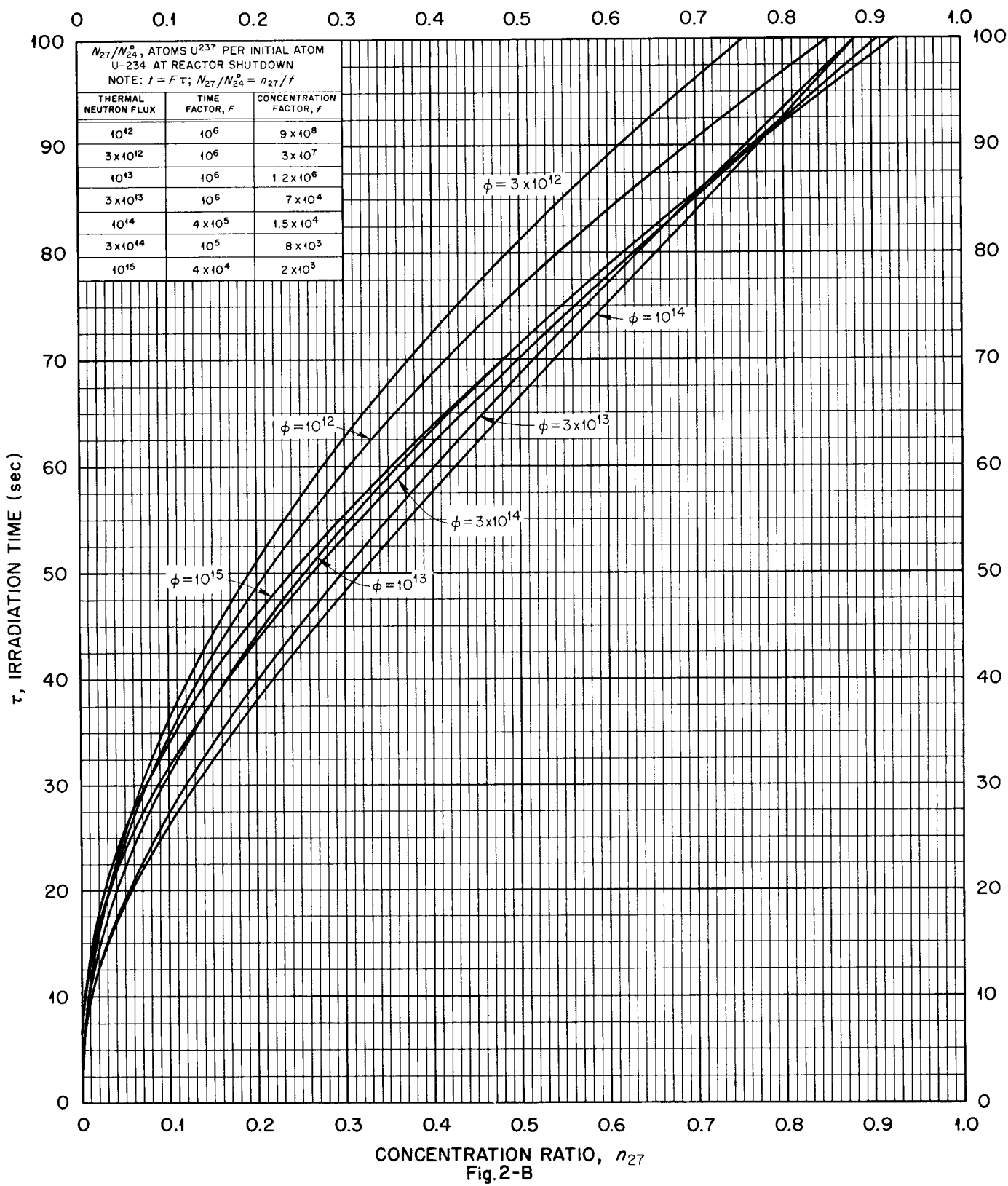
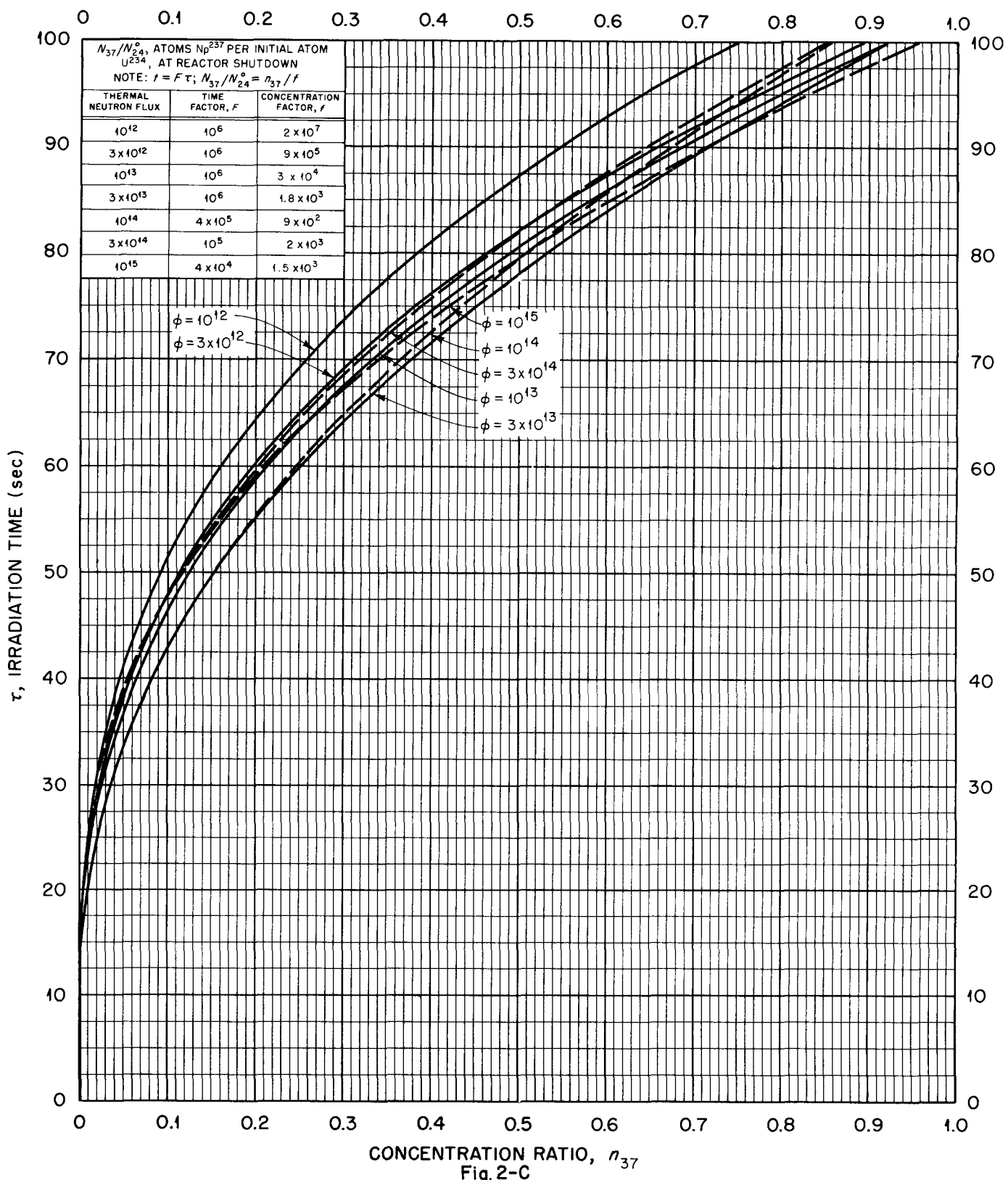
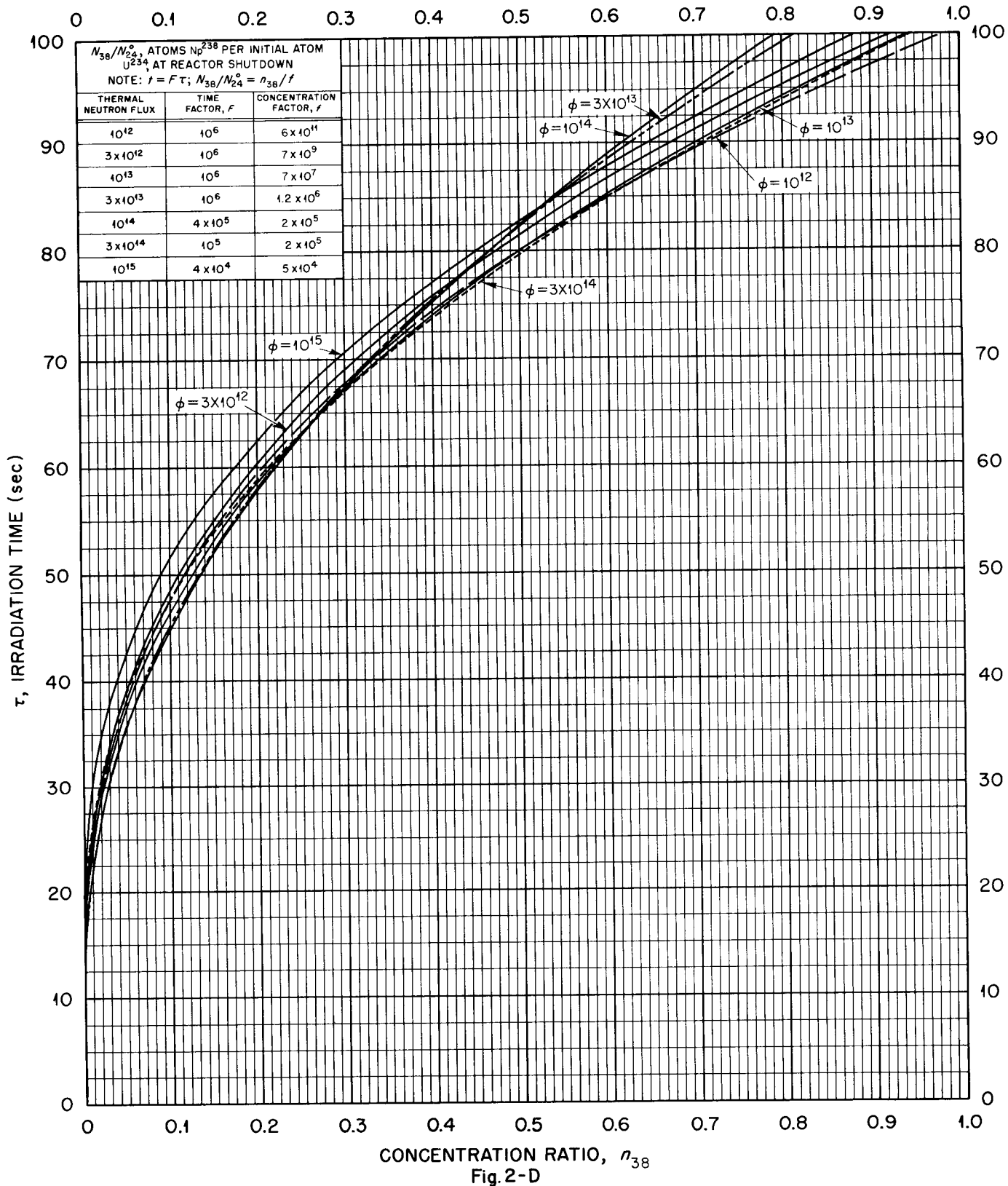


Fig. 2-B





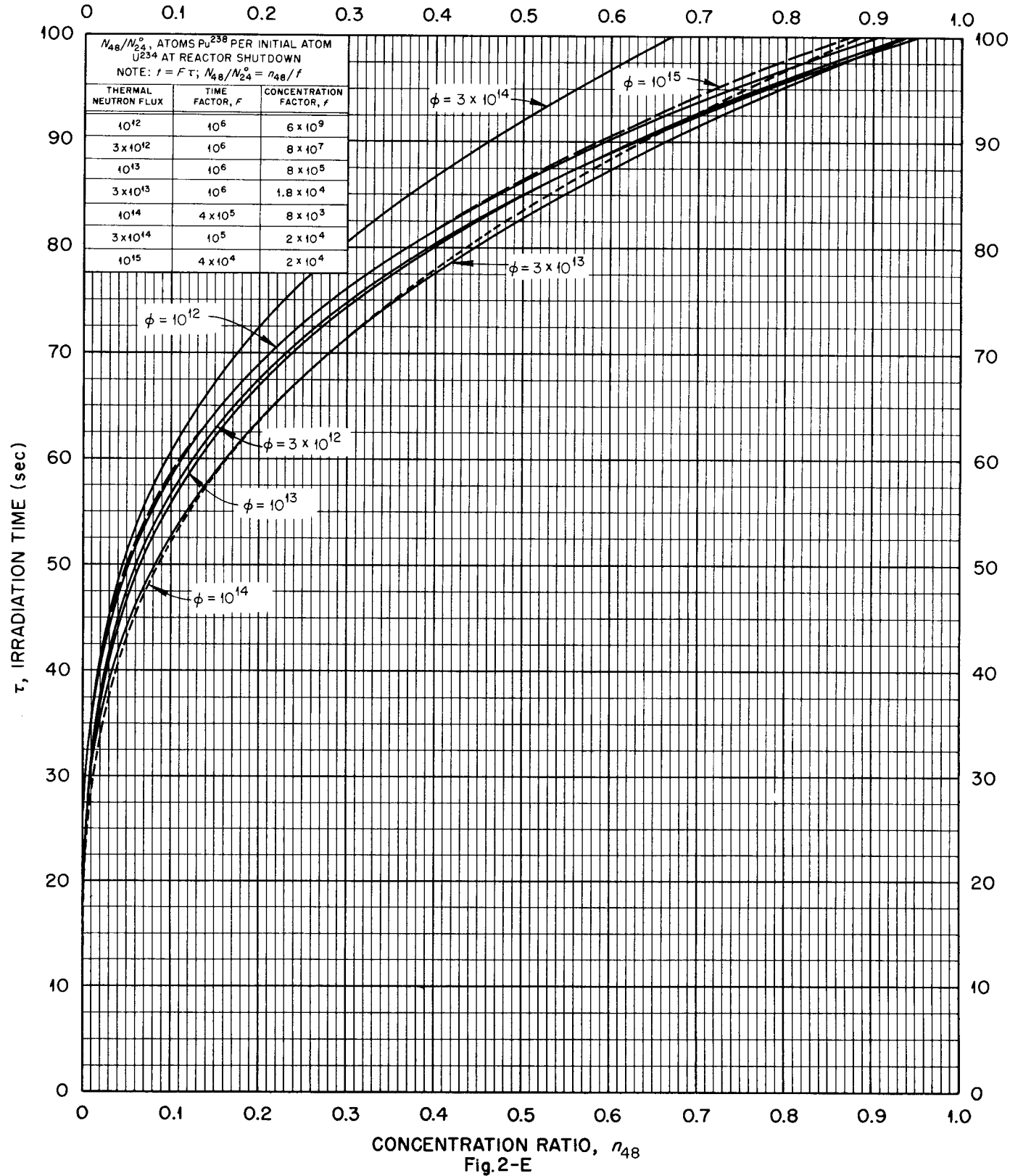


Fig. 2-E

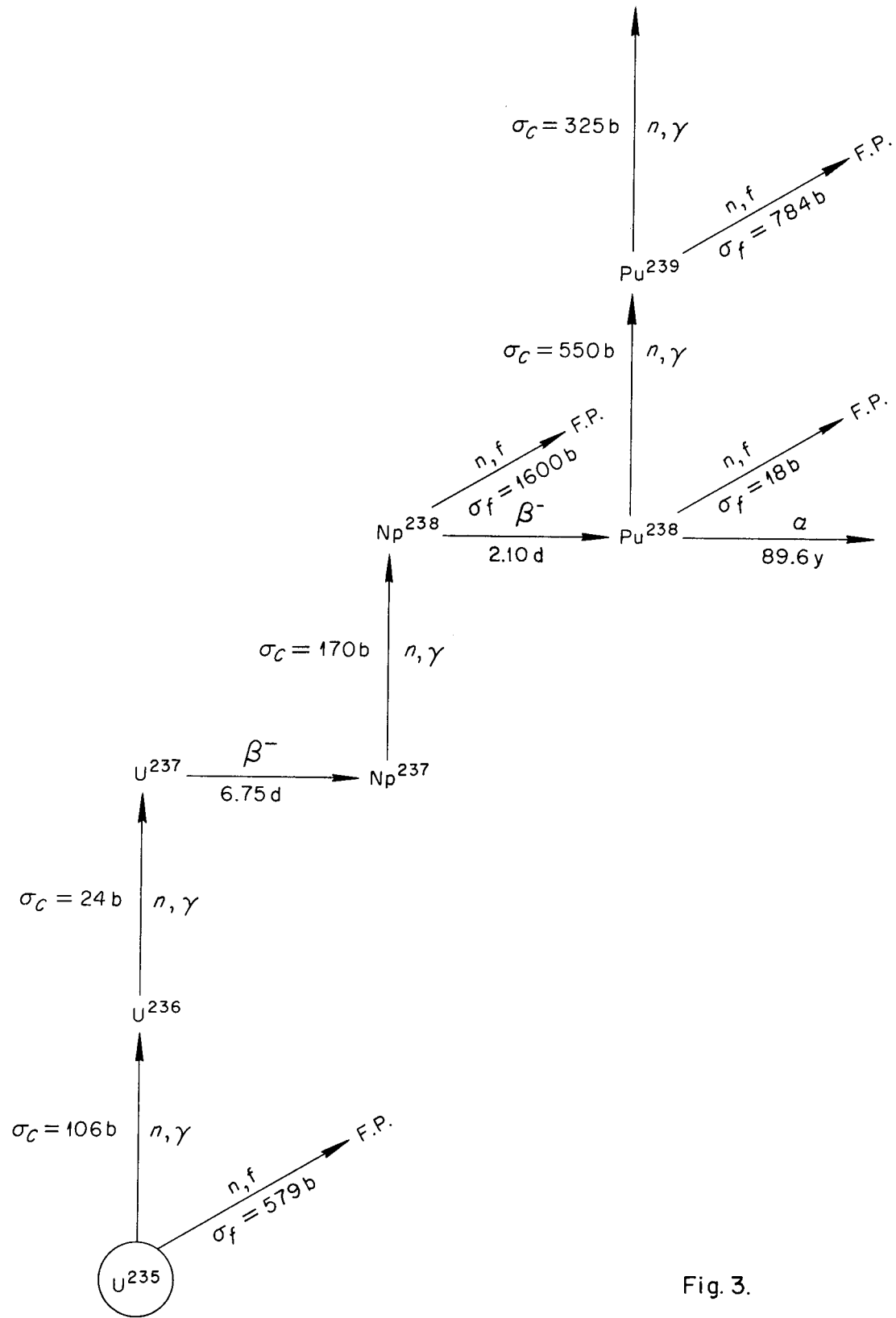


Fig. 3.

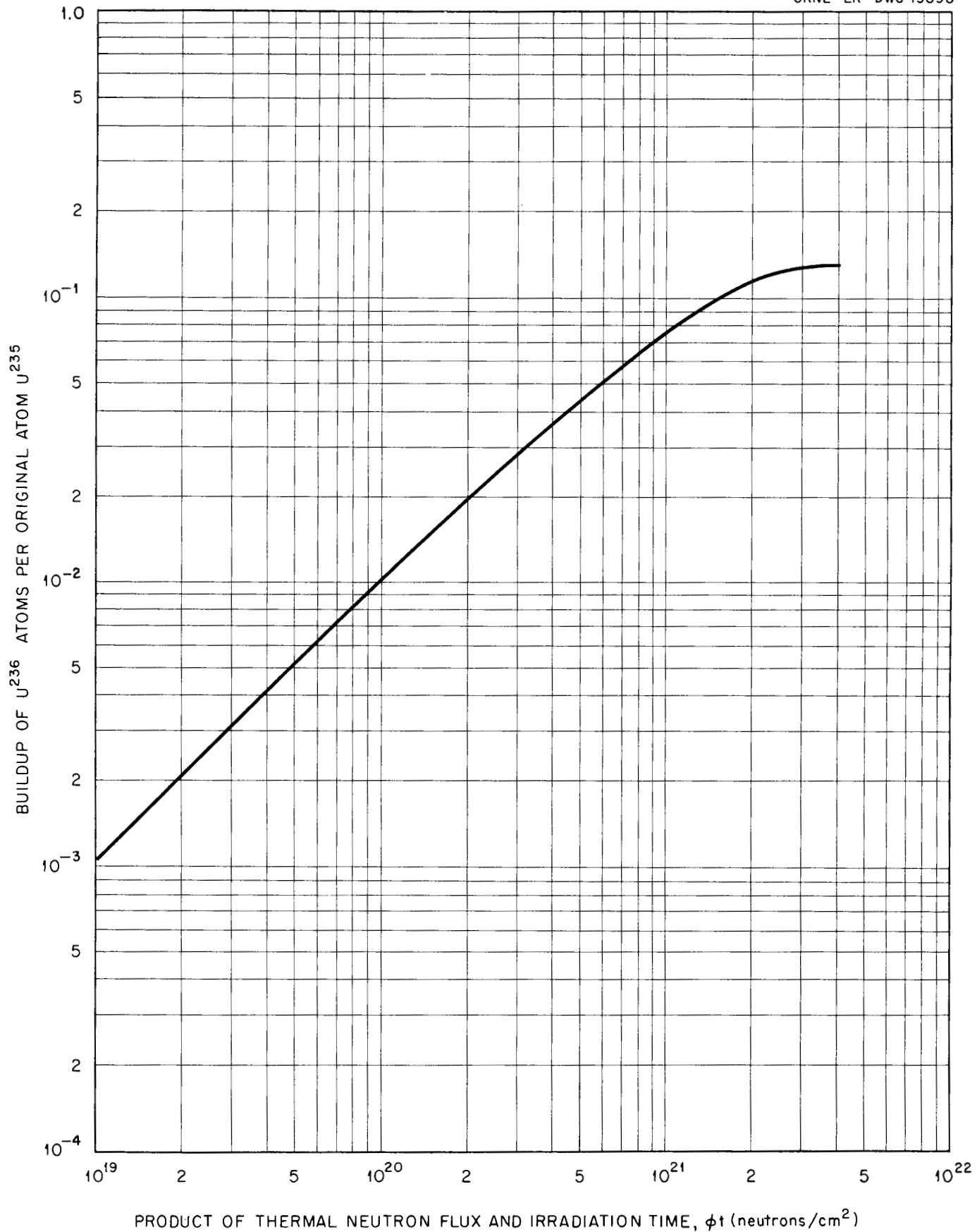


Fig. 3-A. Buildup of U²³⁶ from U²³⁵ as a Function of the Product of Irradiation Time and Thermal Neutron Flux.

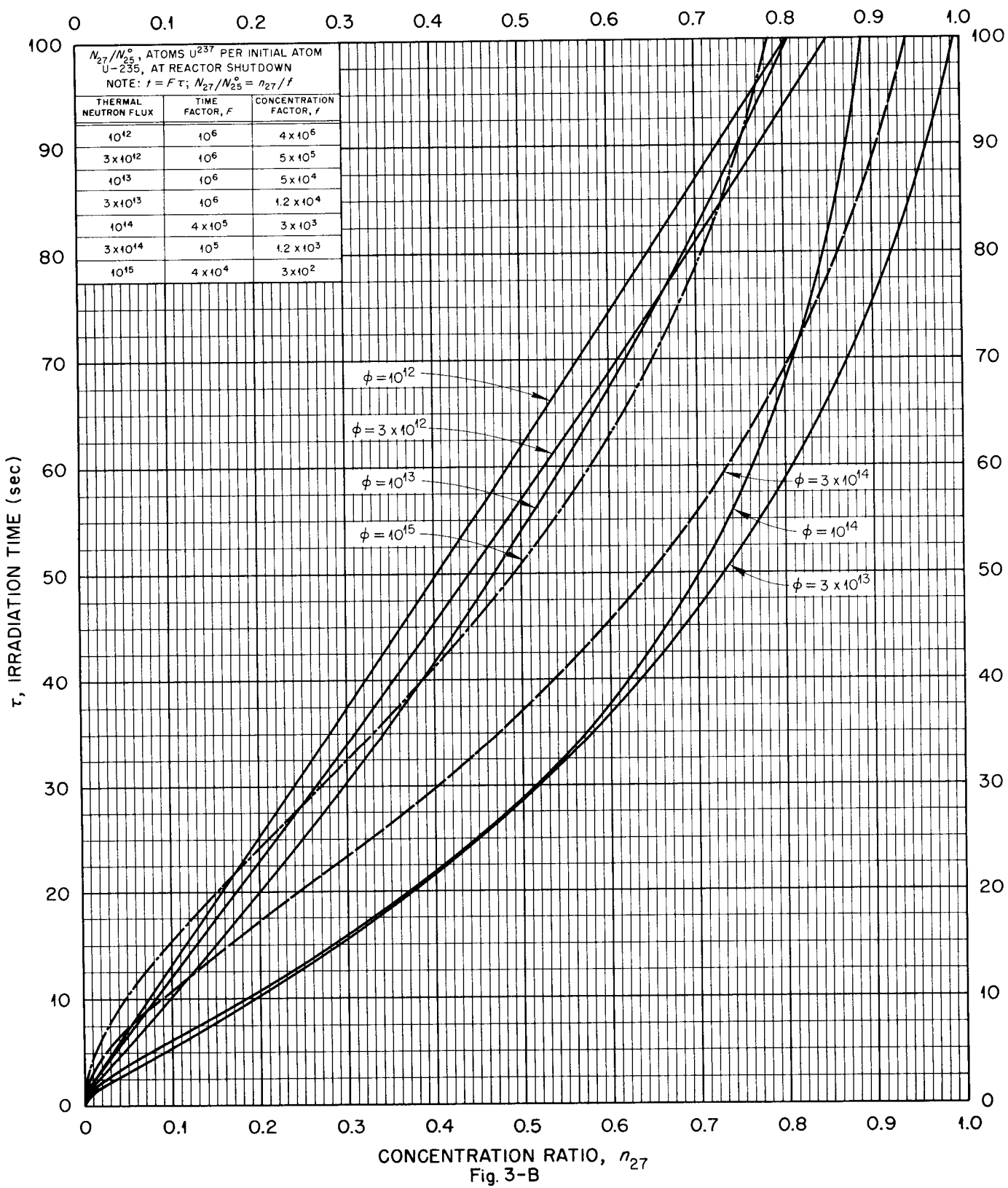


Fig. 3-B

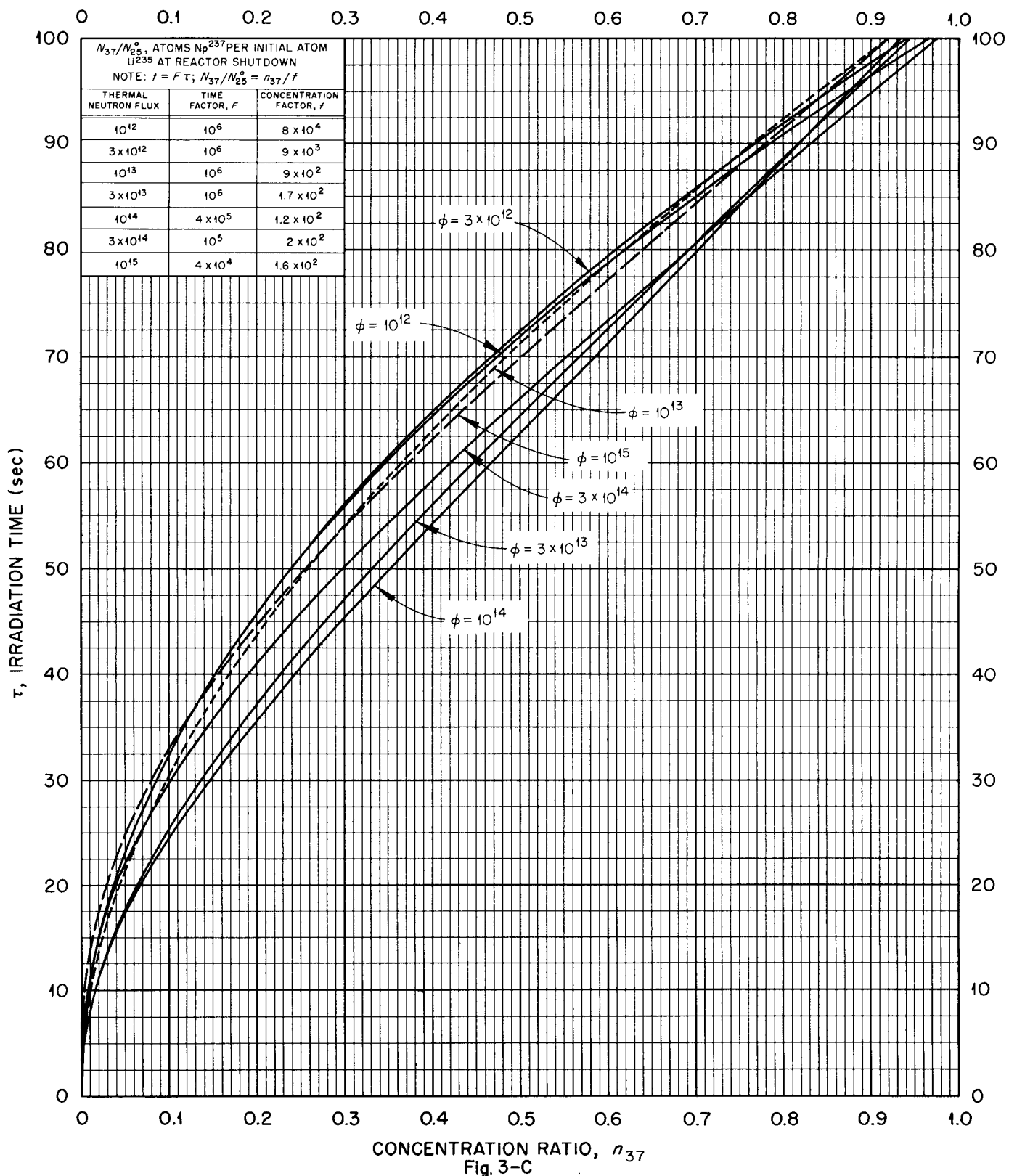
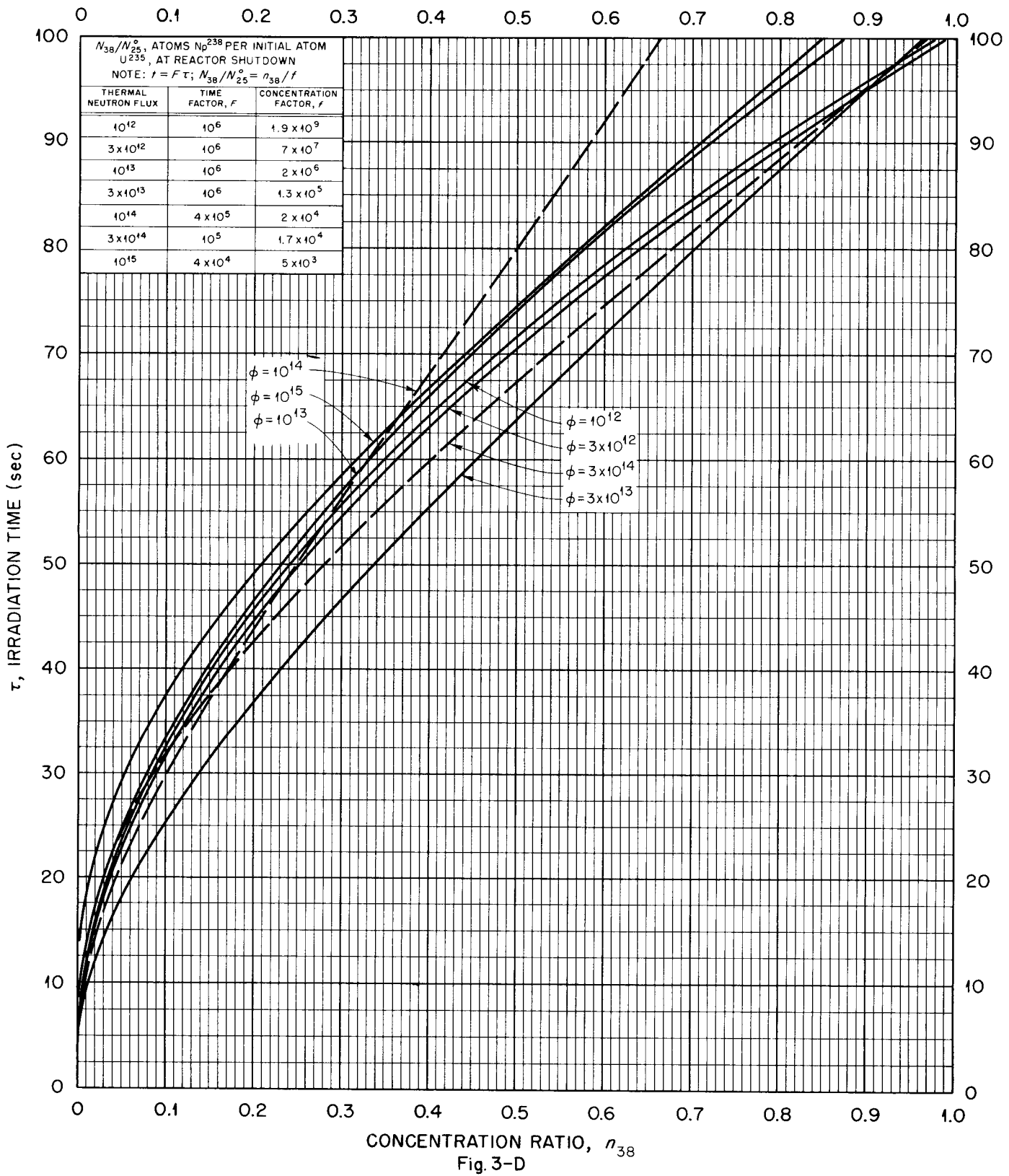


Fig. 3-C



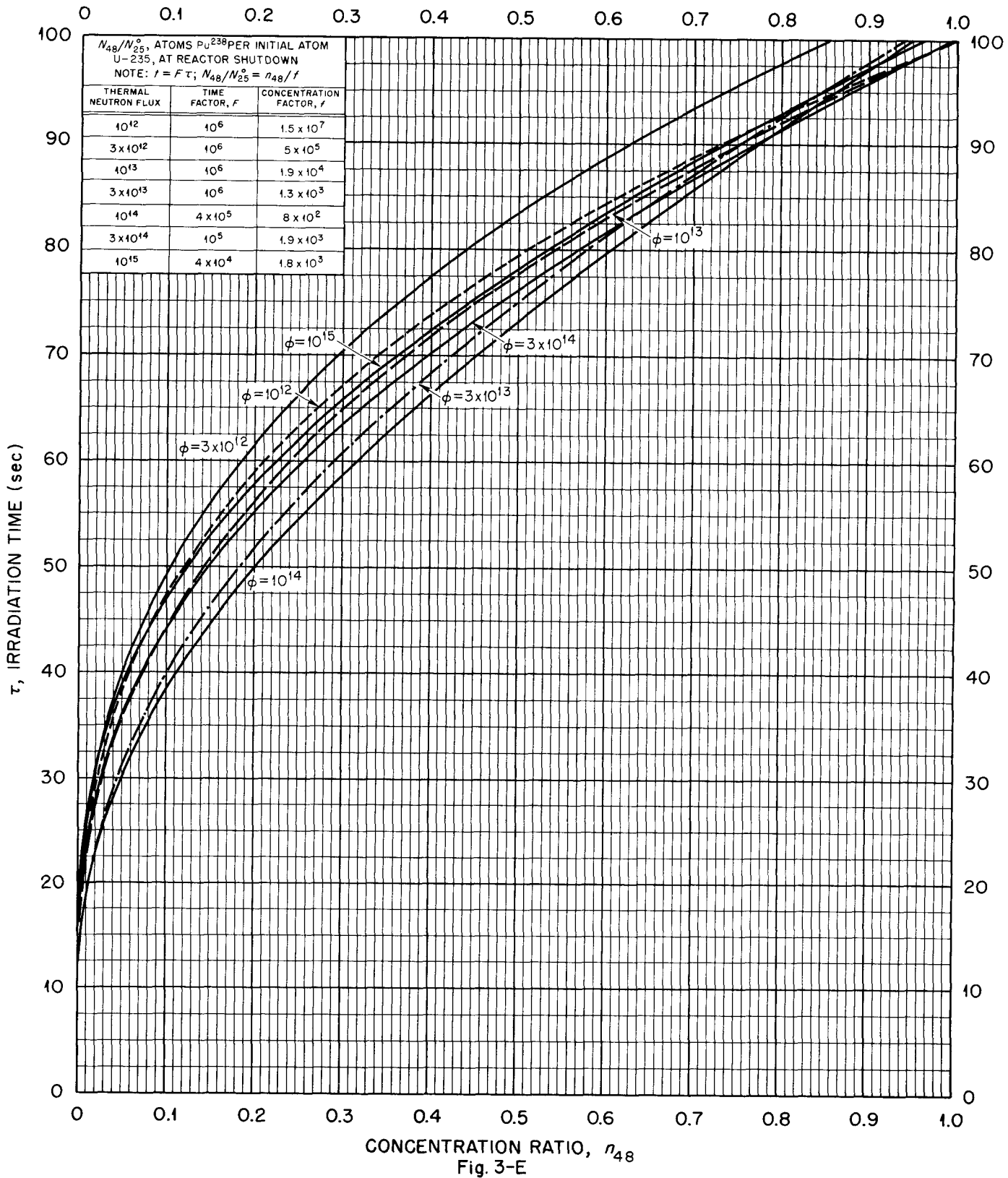
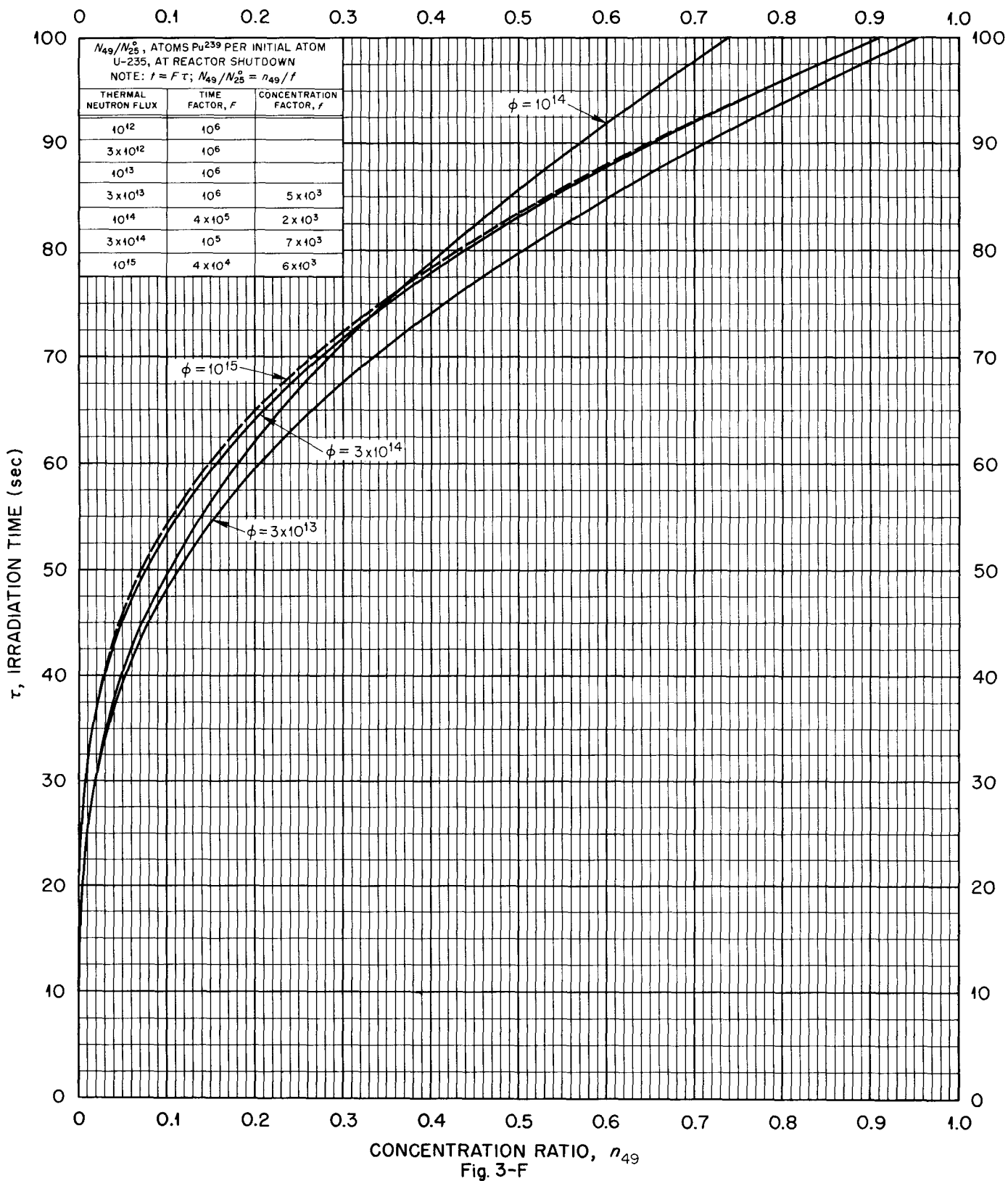


Fig. 3-E



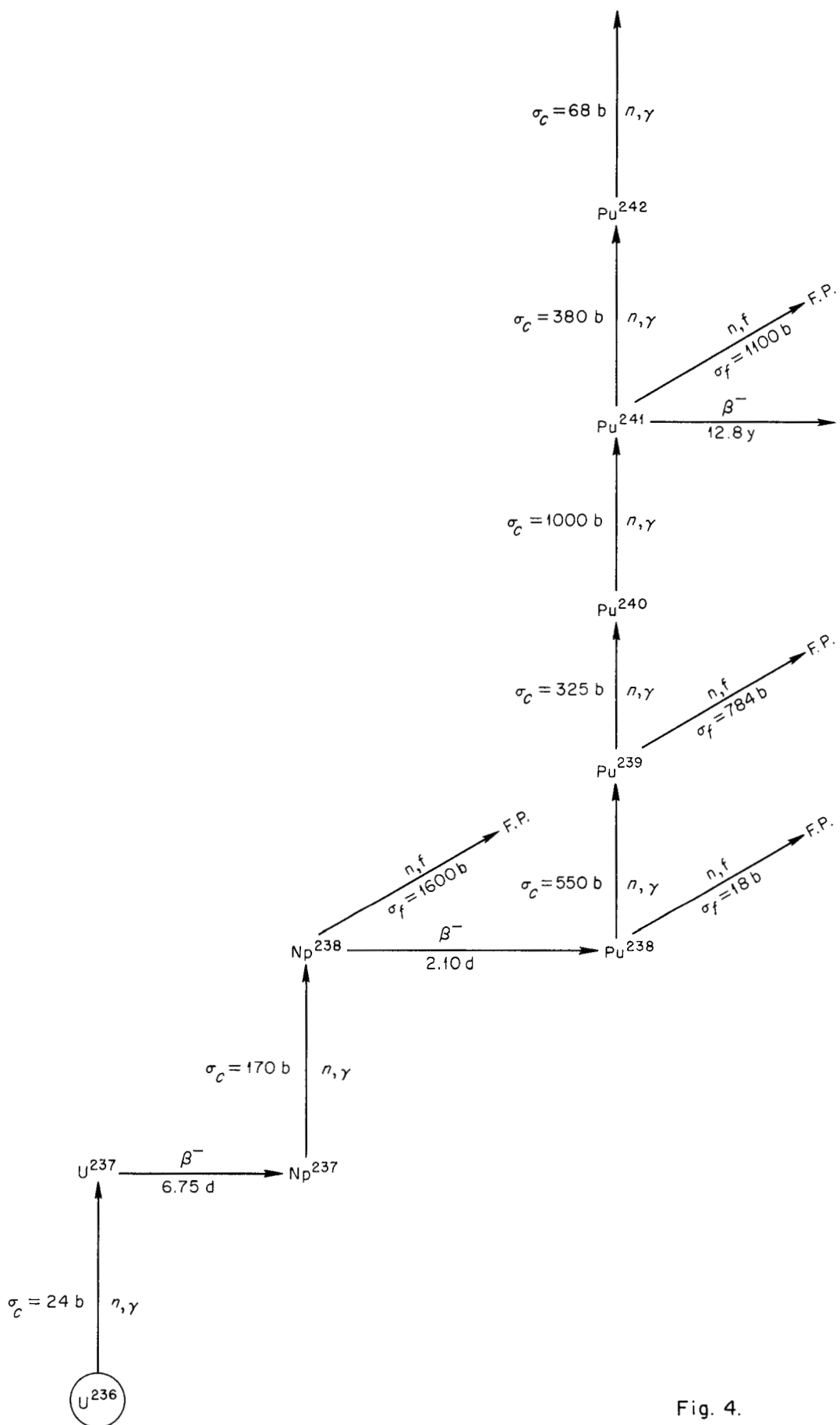


Fig. 4.

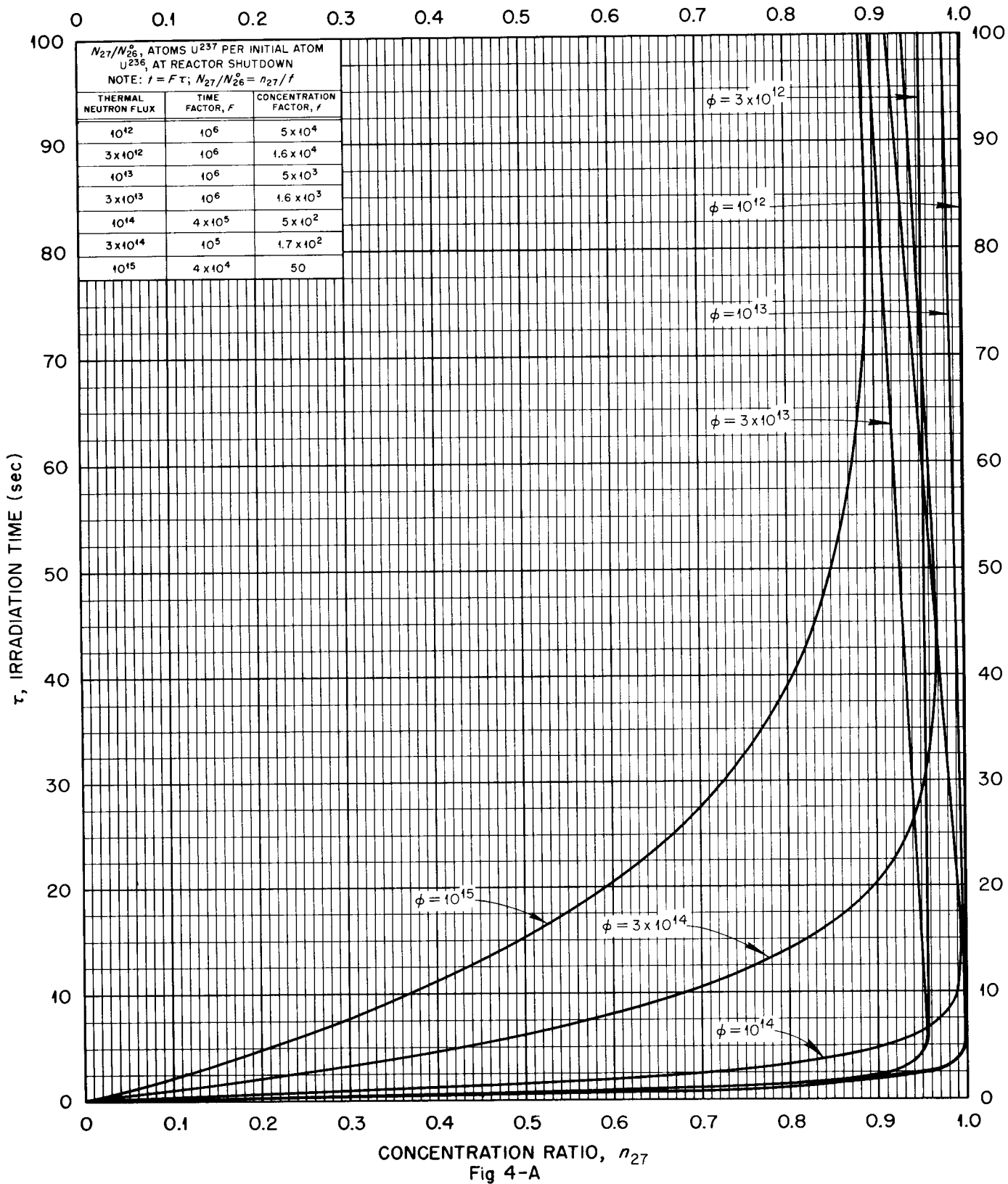


Fig 4-A

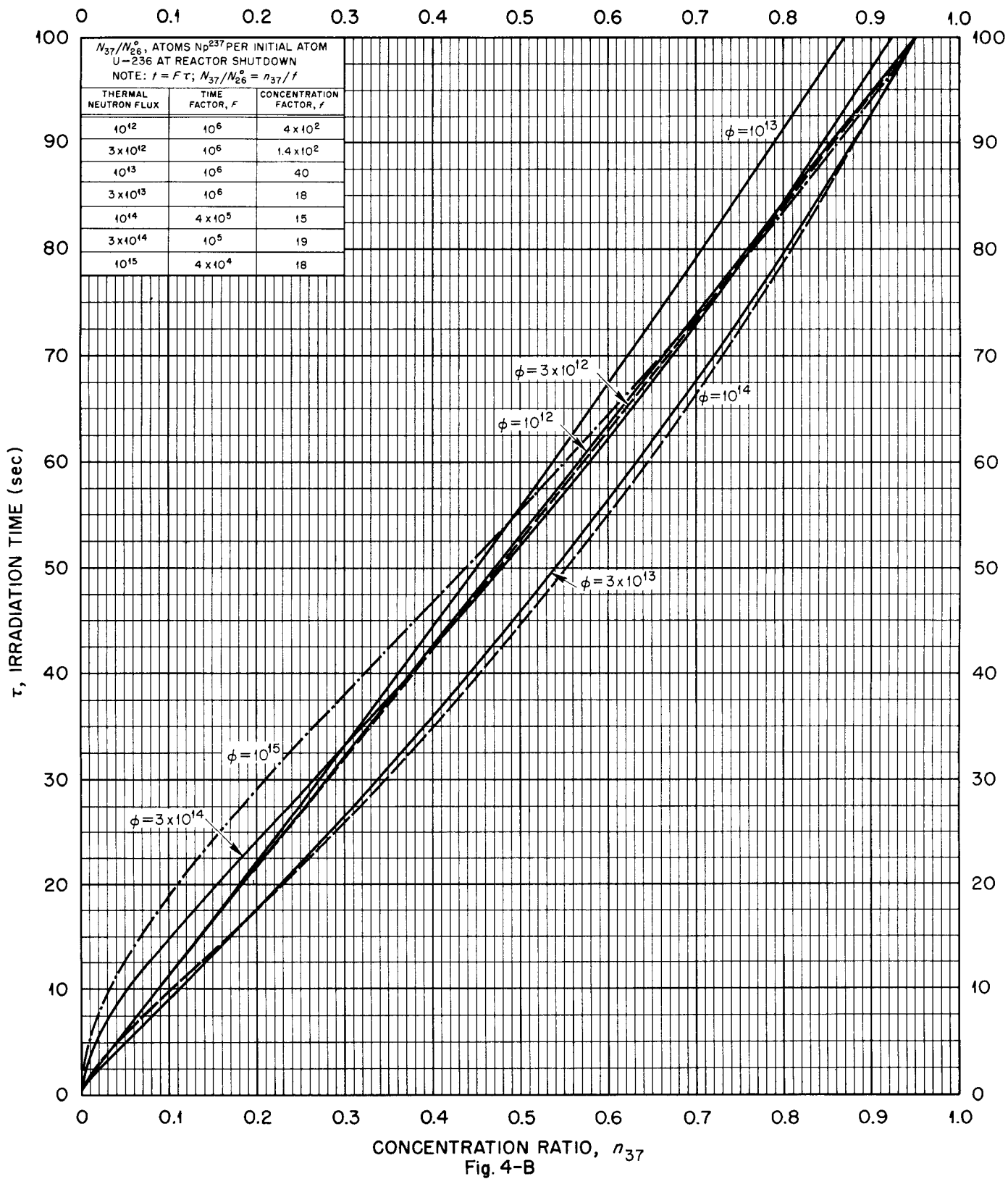
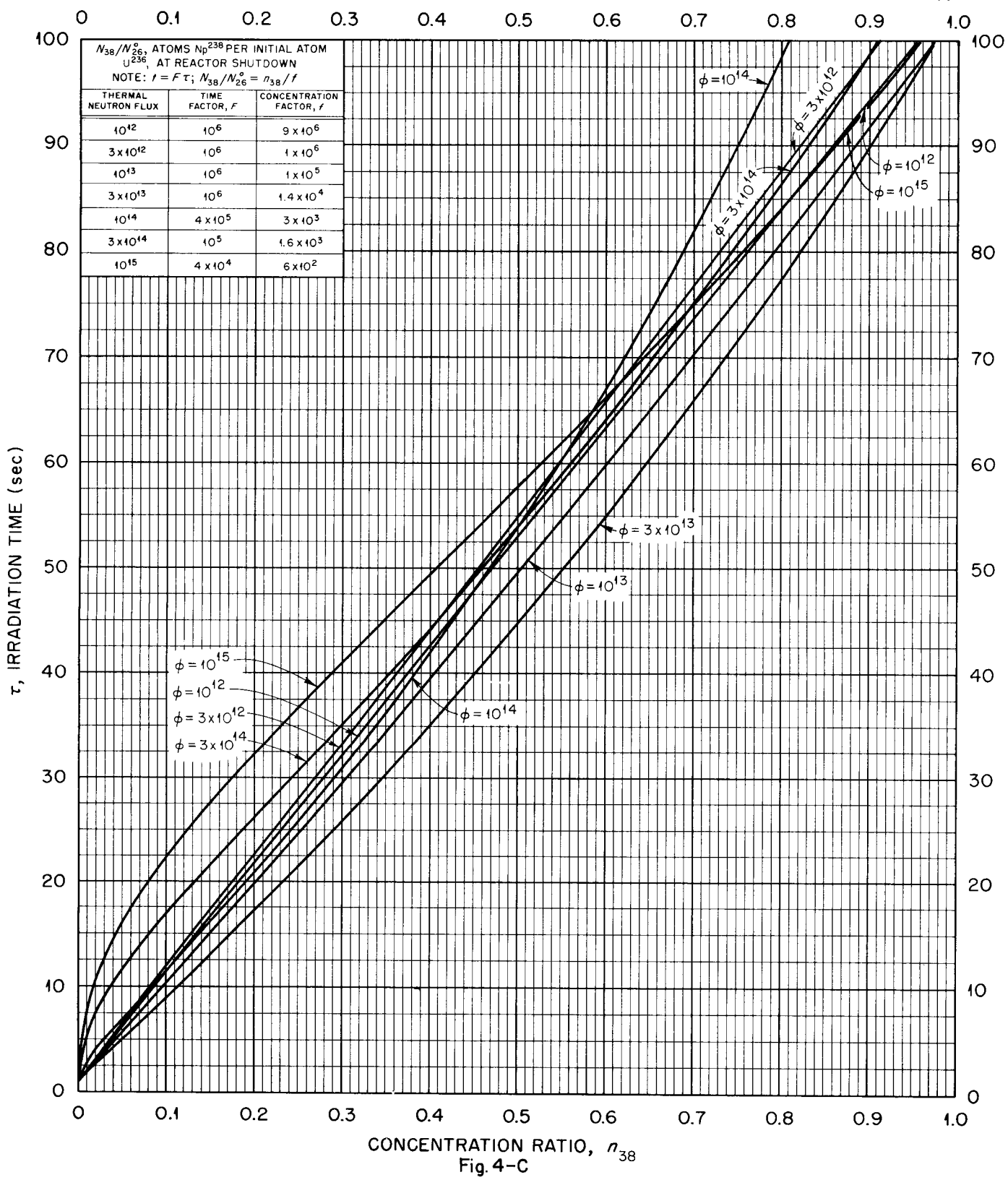
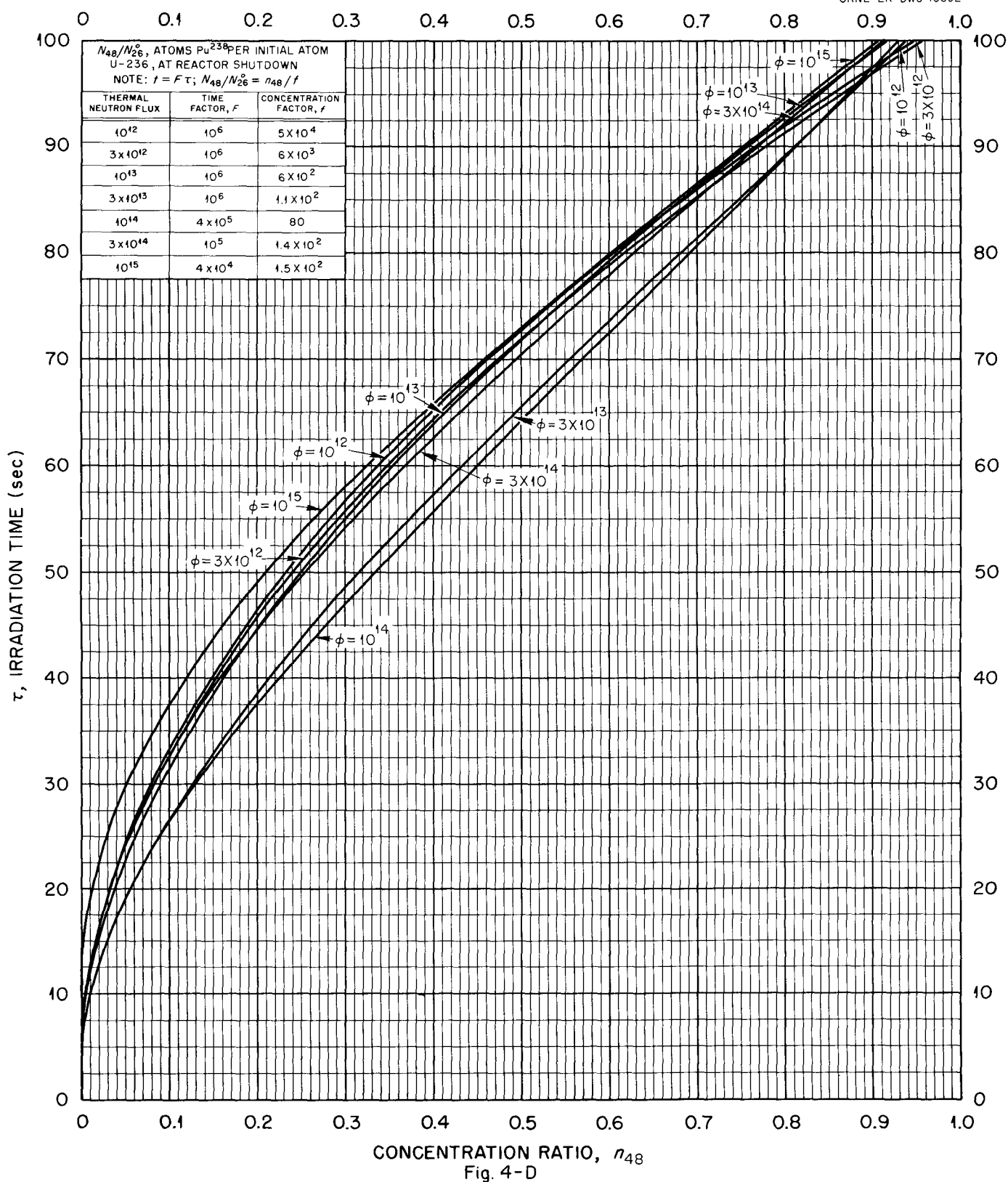


Fig. 4-B





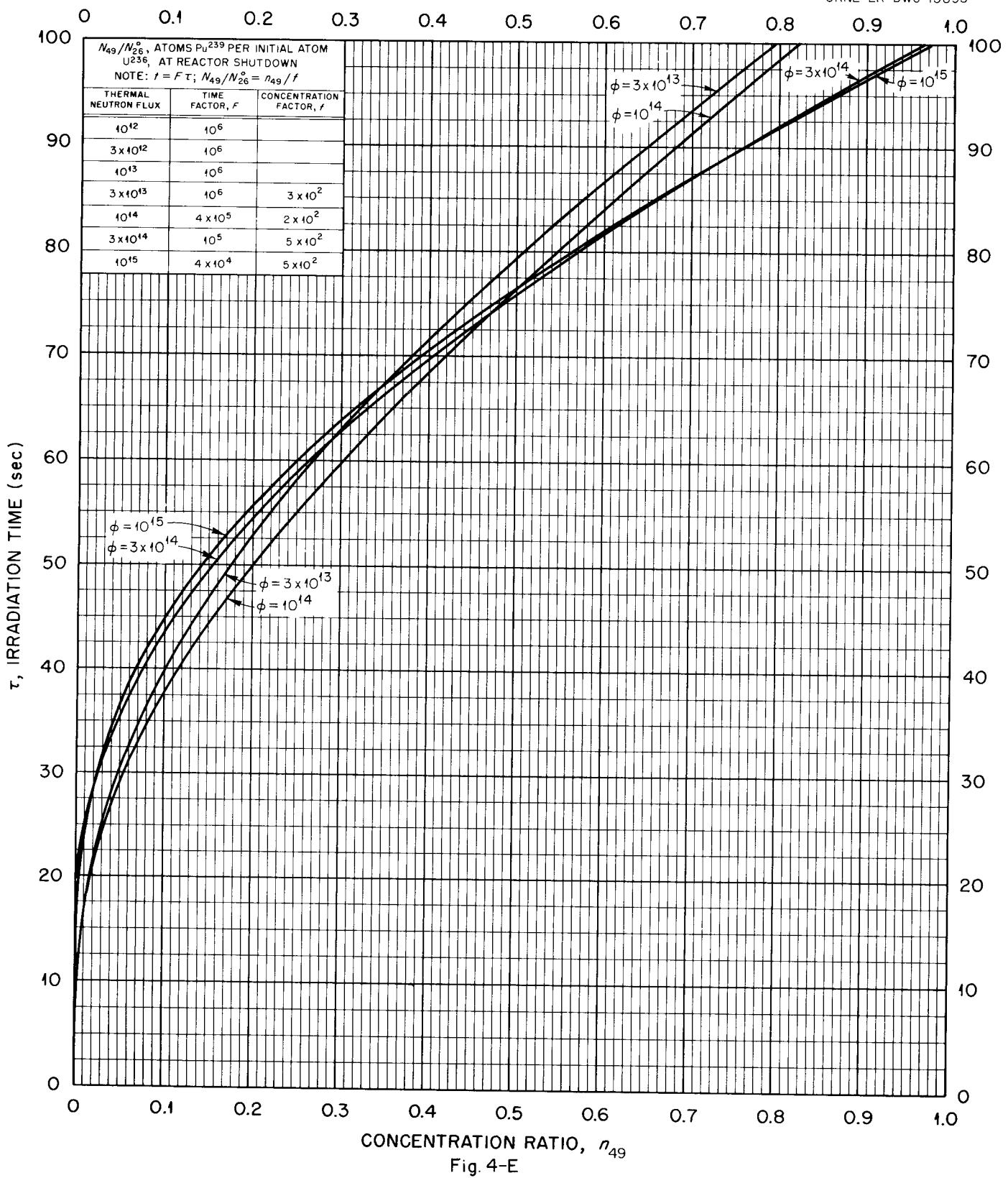
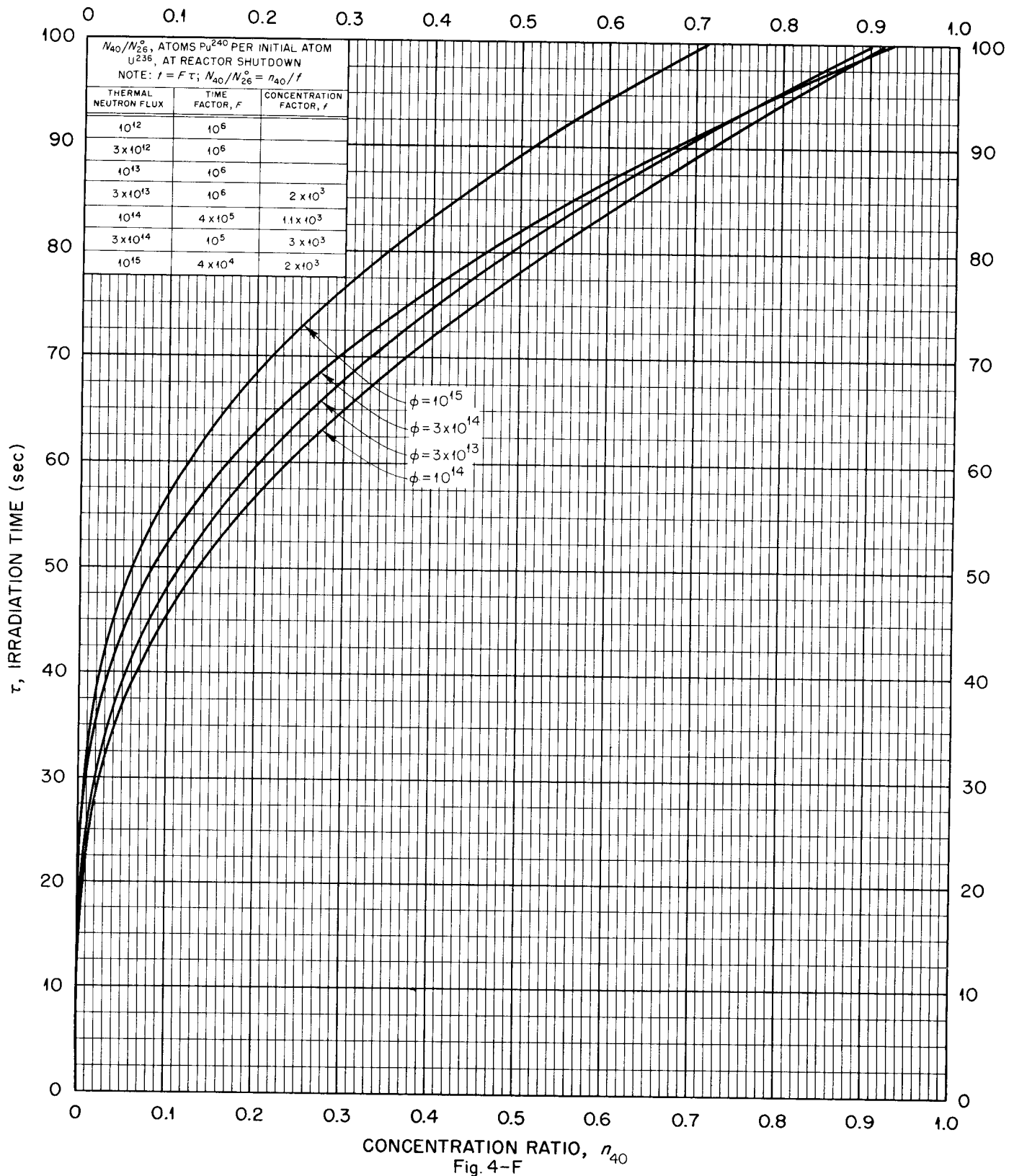
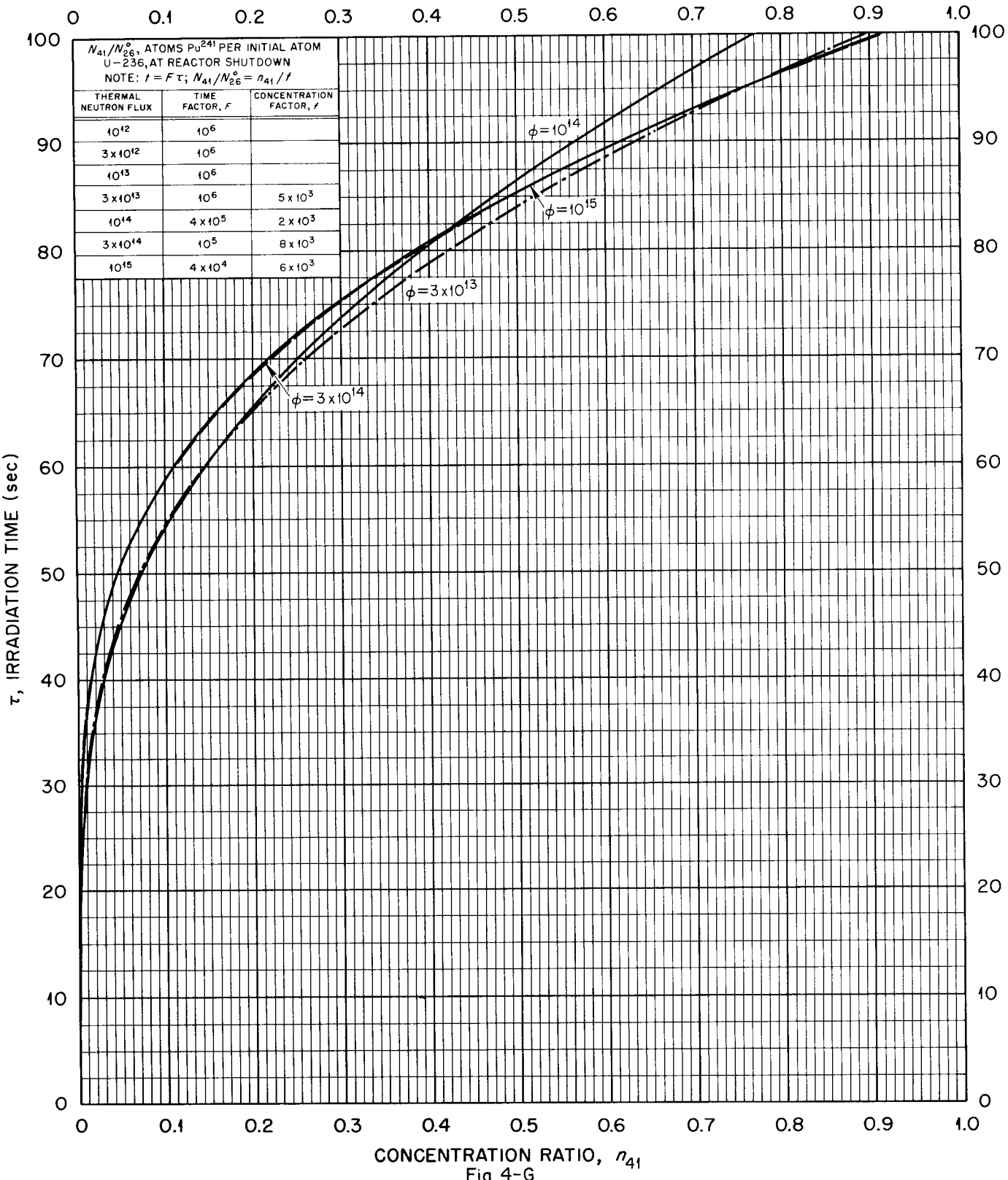
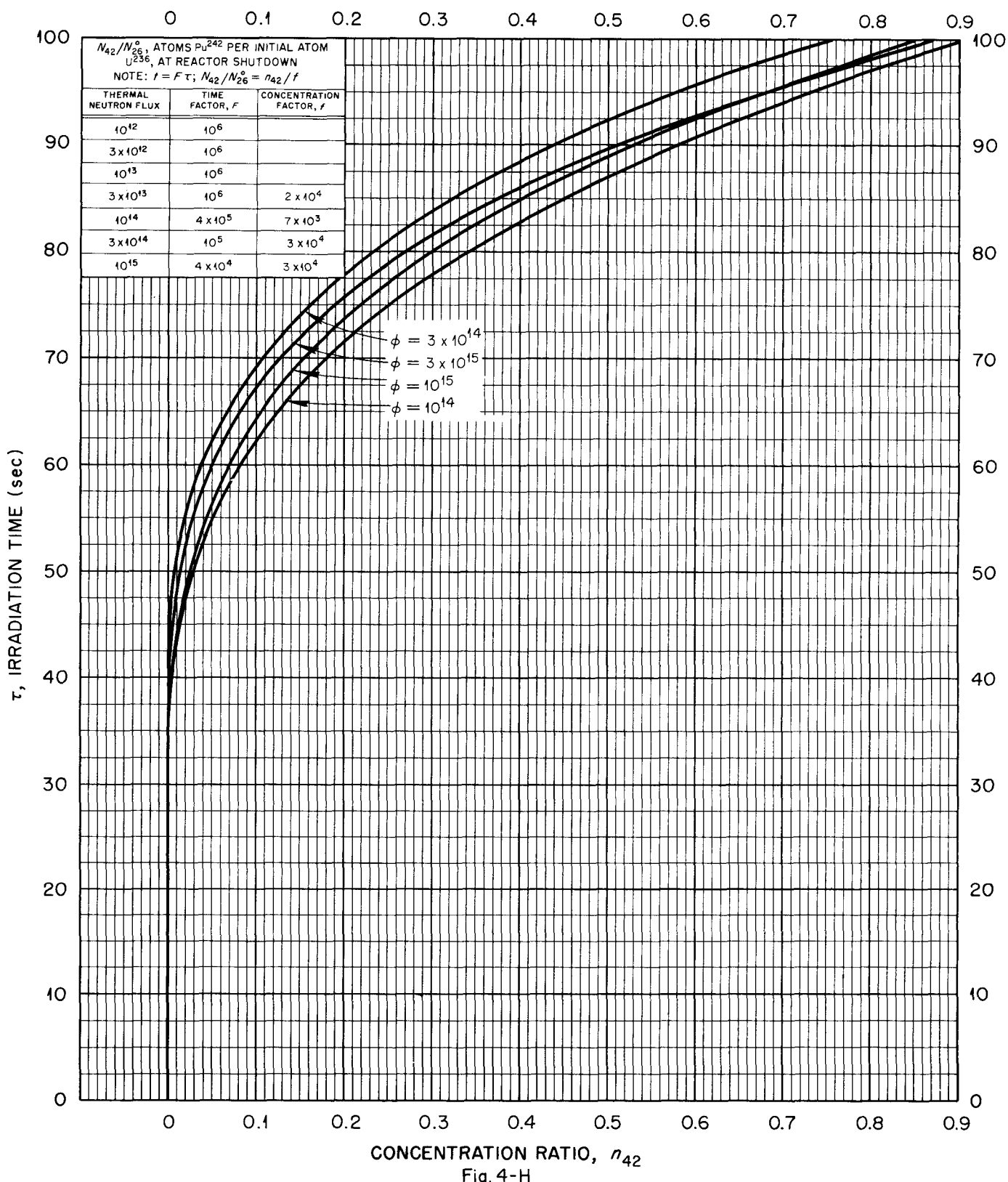


Fig. 4-E







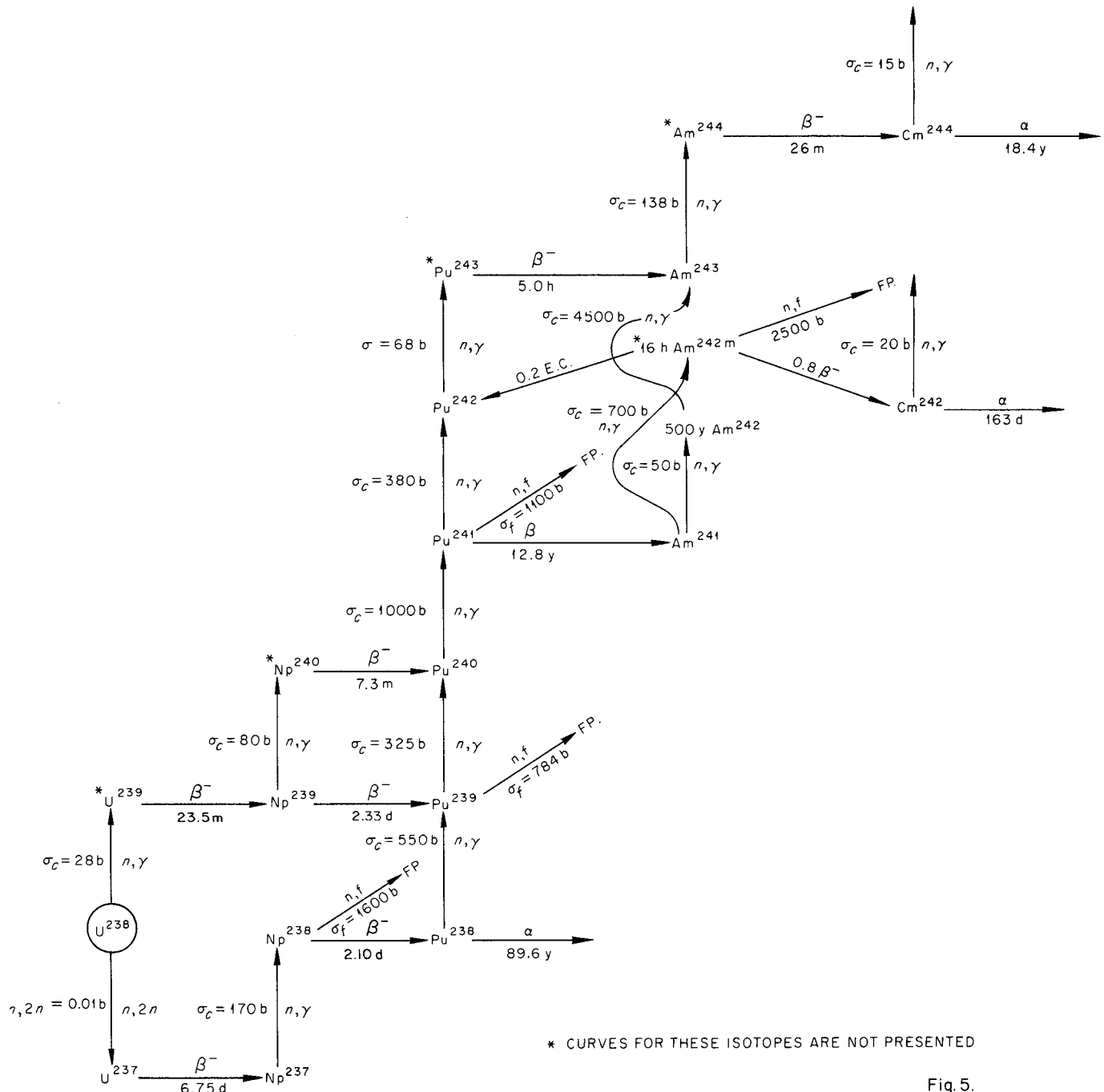
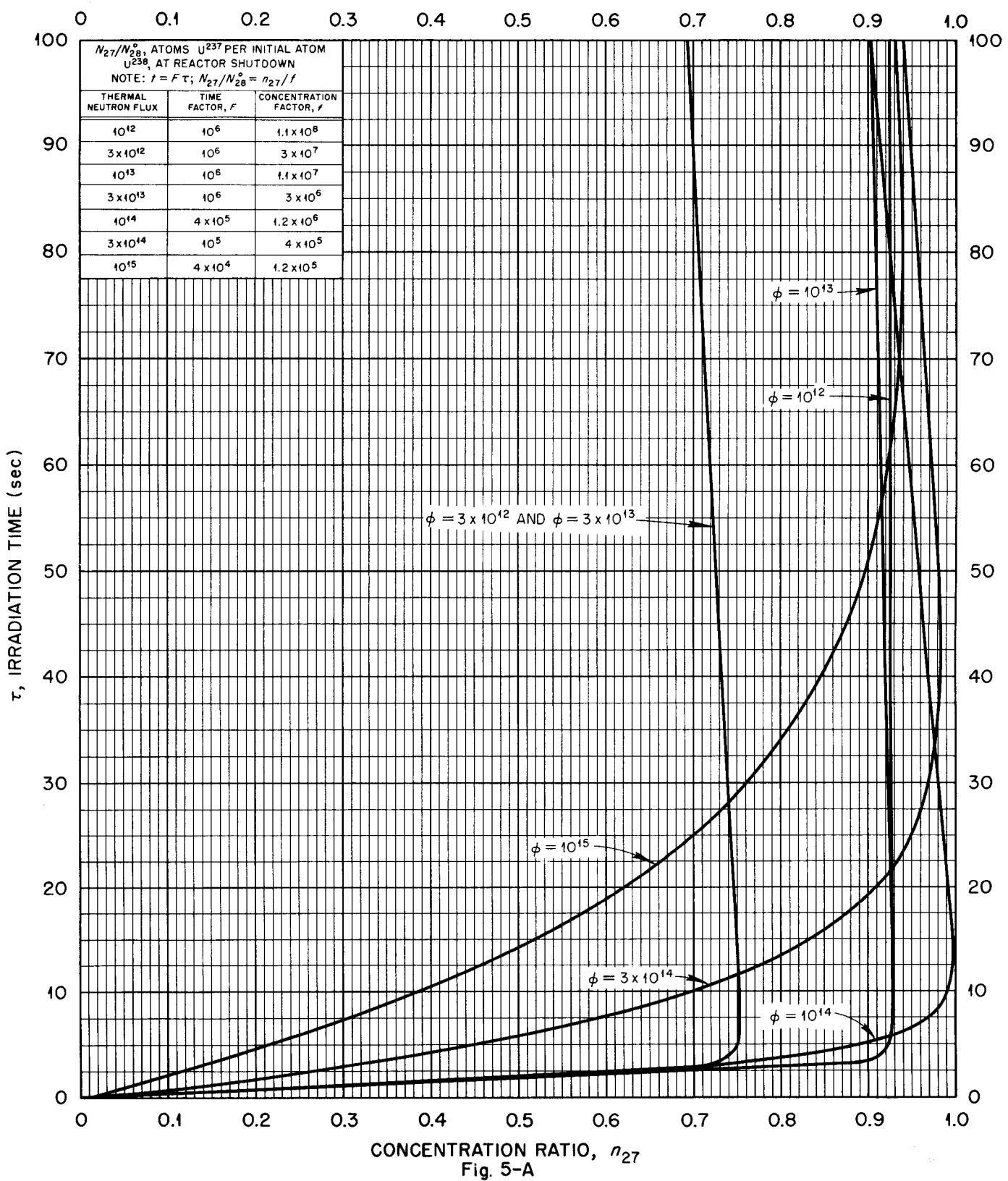


Fig. 5.



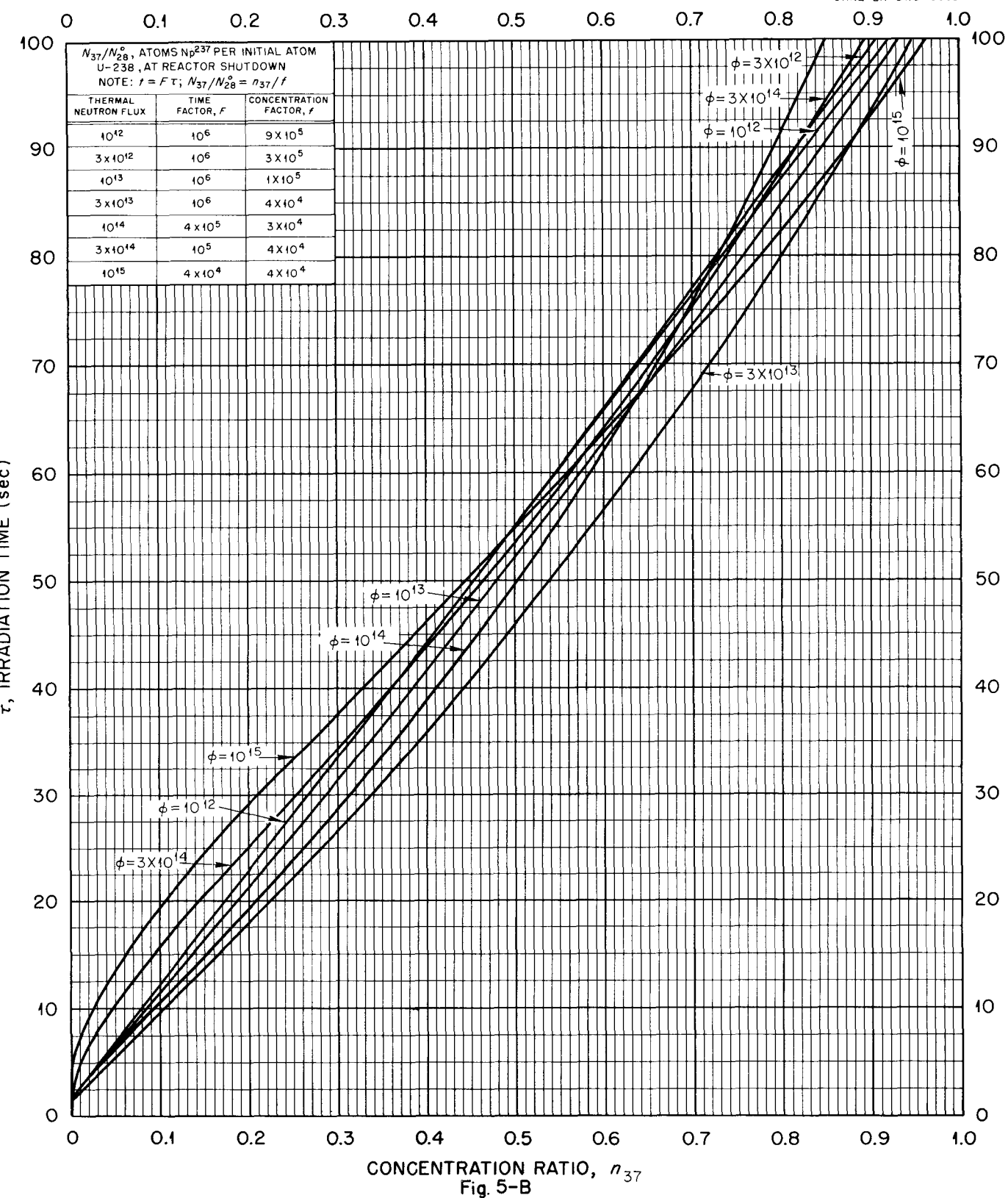


Fig. 5-B

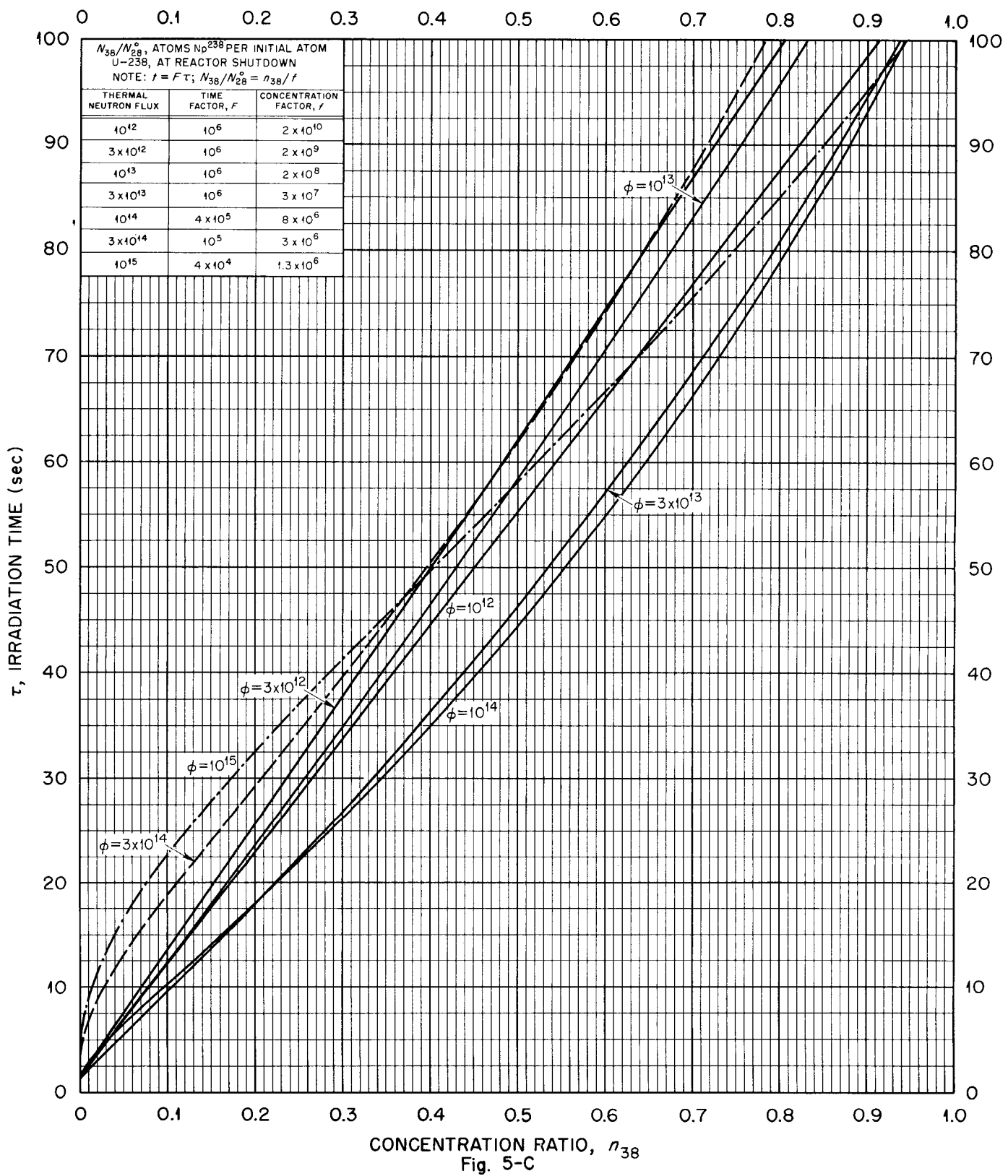
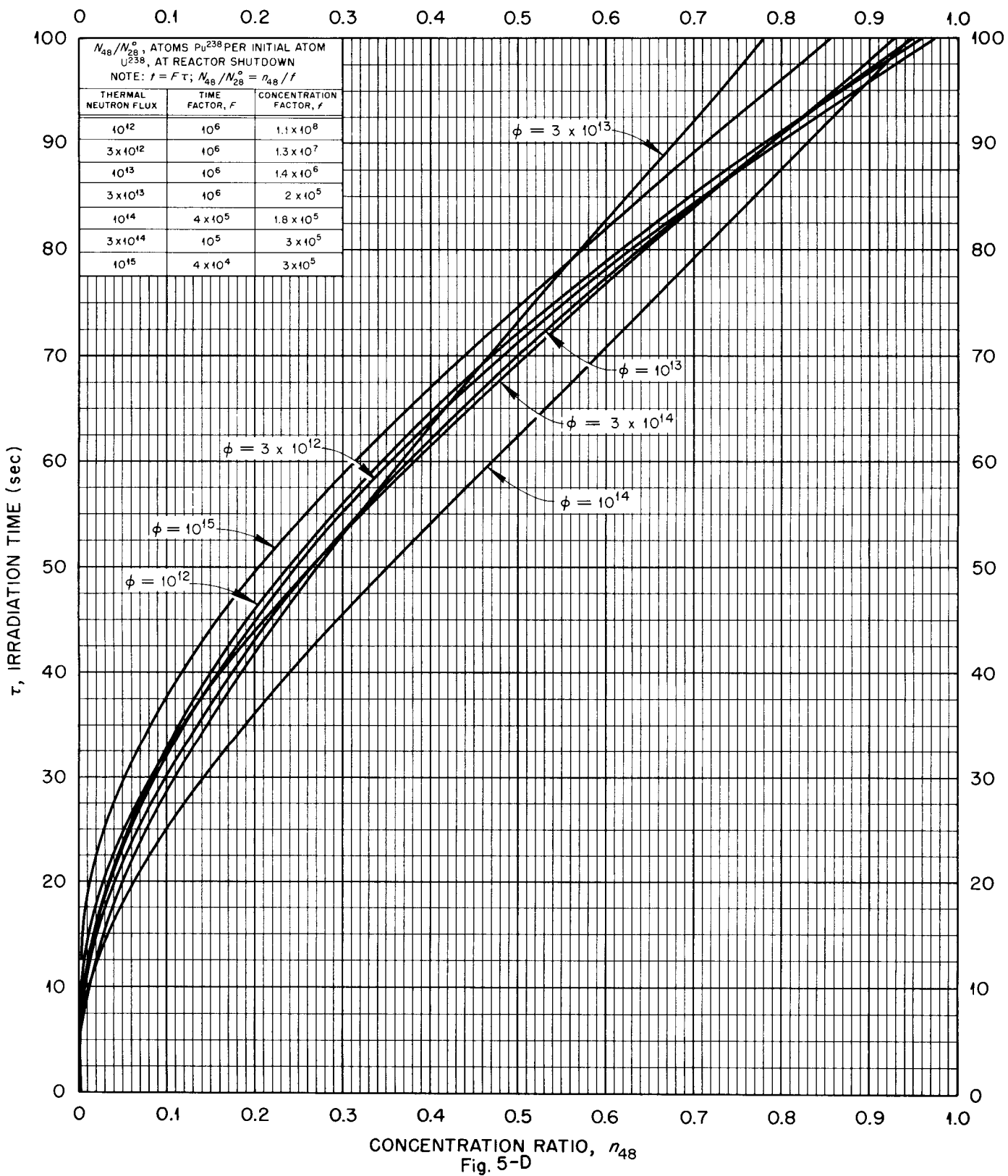


Fig. 5-C



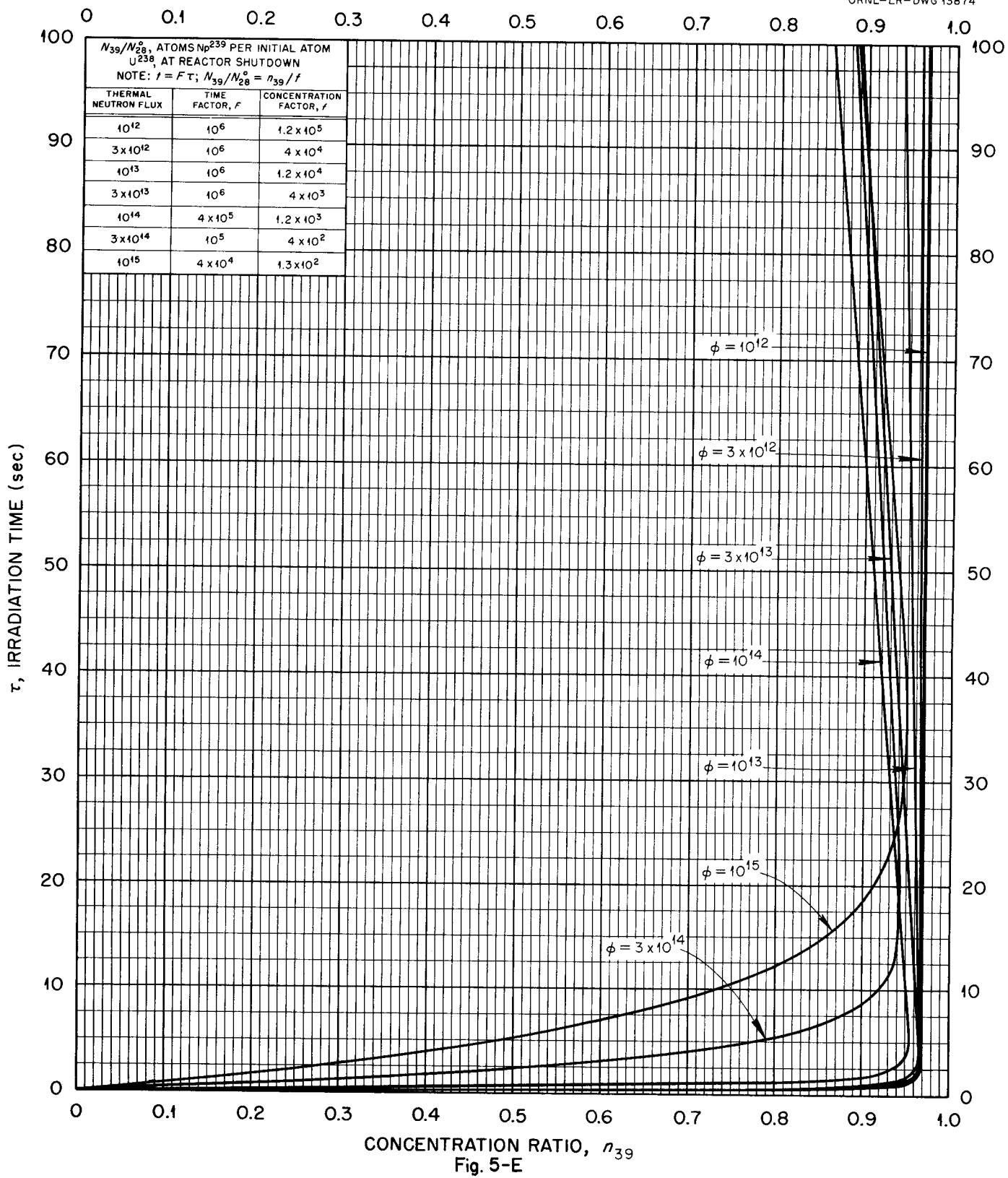
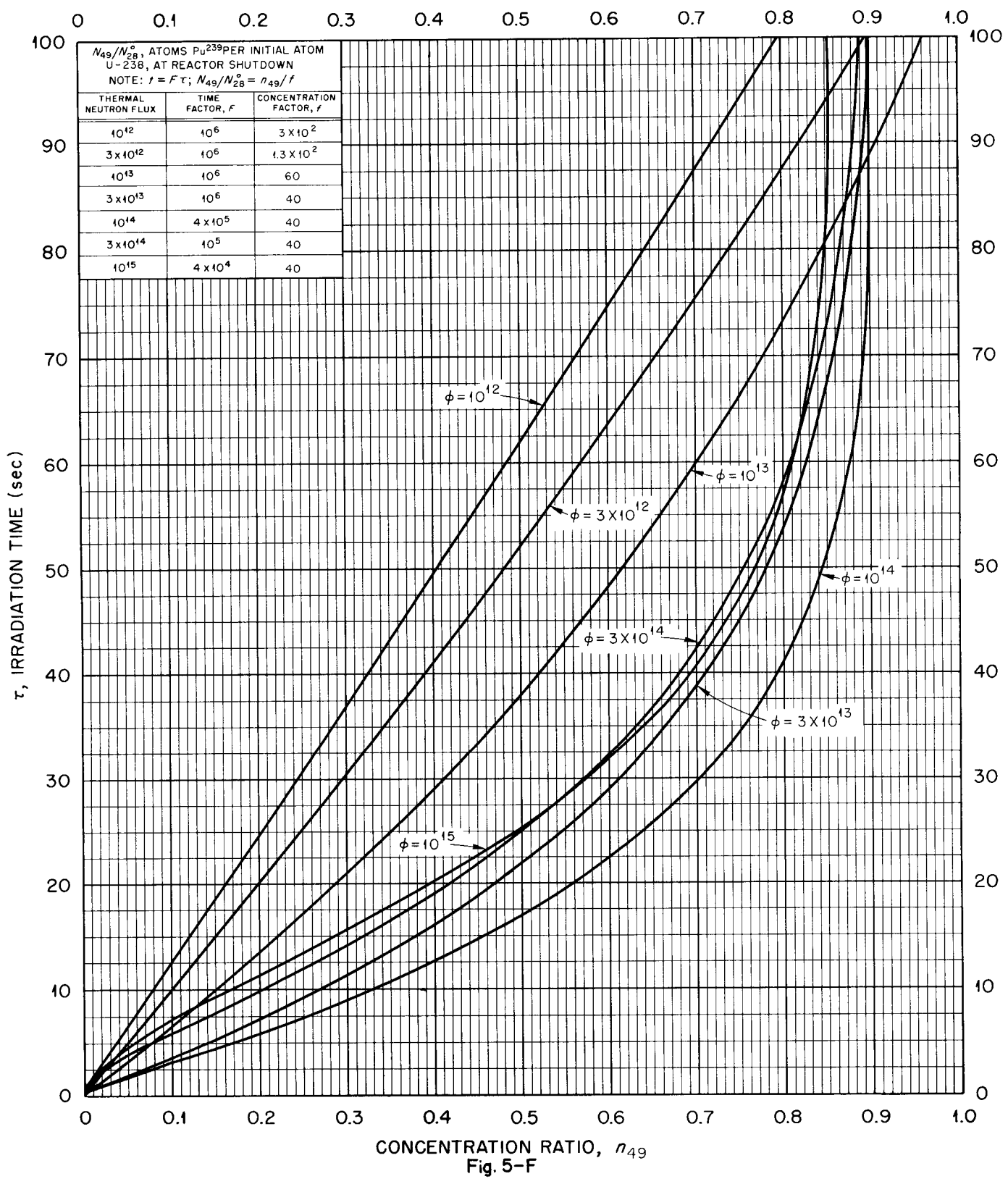


Fig. 5-E



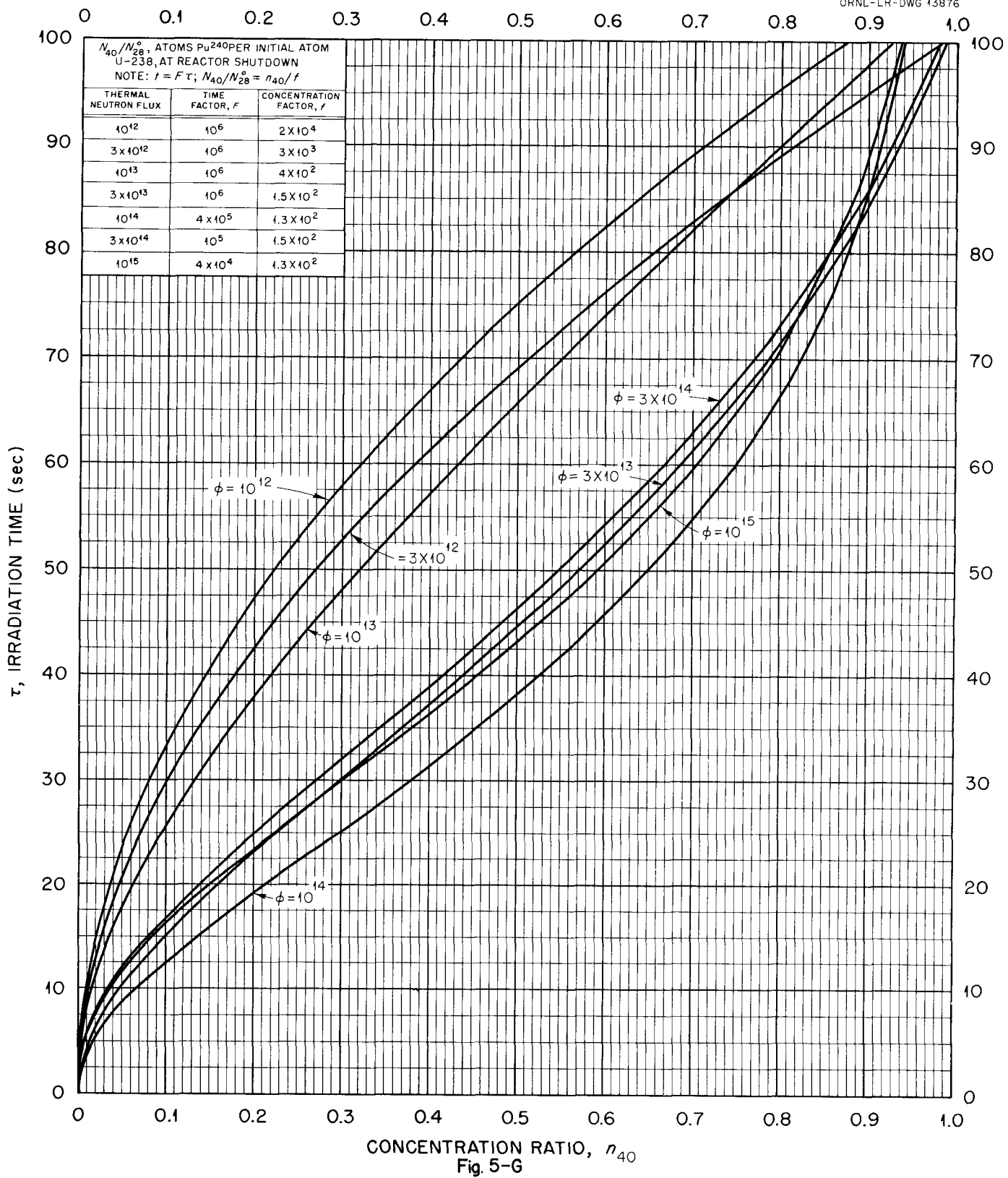
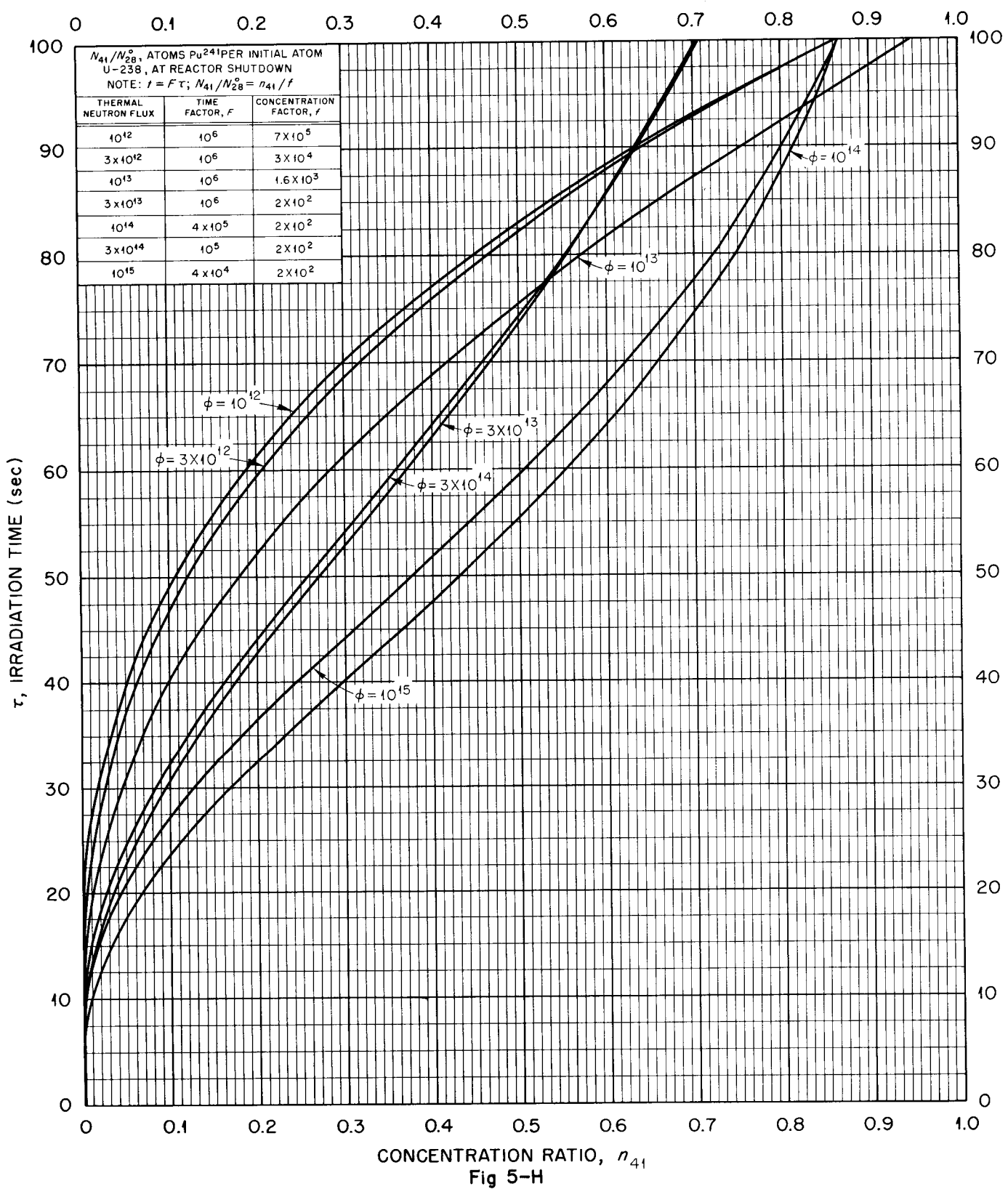


Fig. 5-G

CONCENTRATION RATIO, n_{41}
Fig 5-H

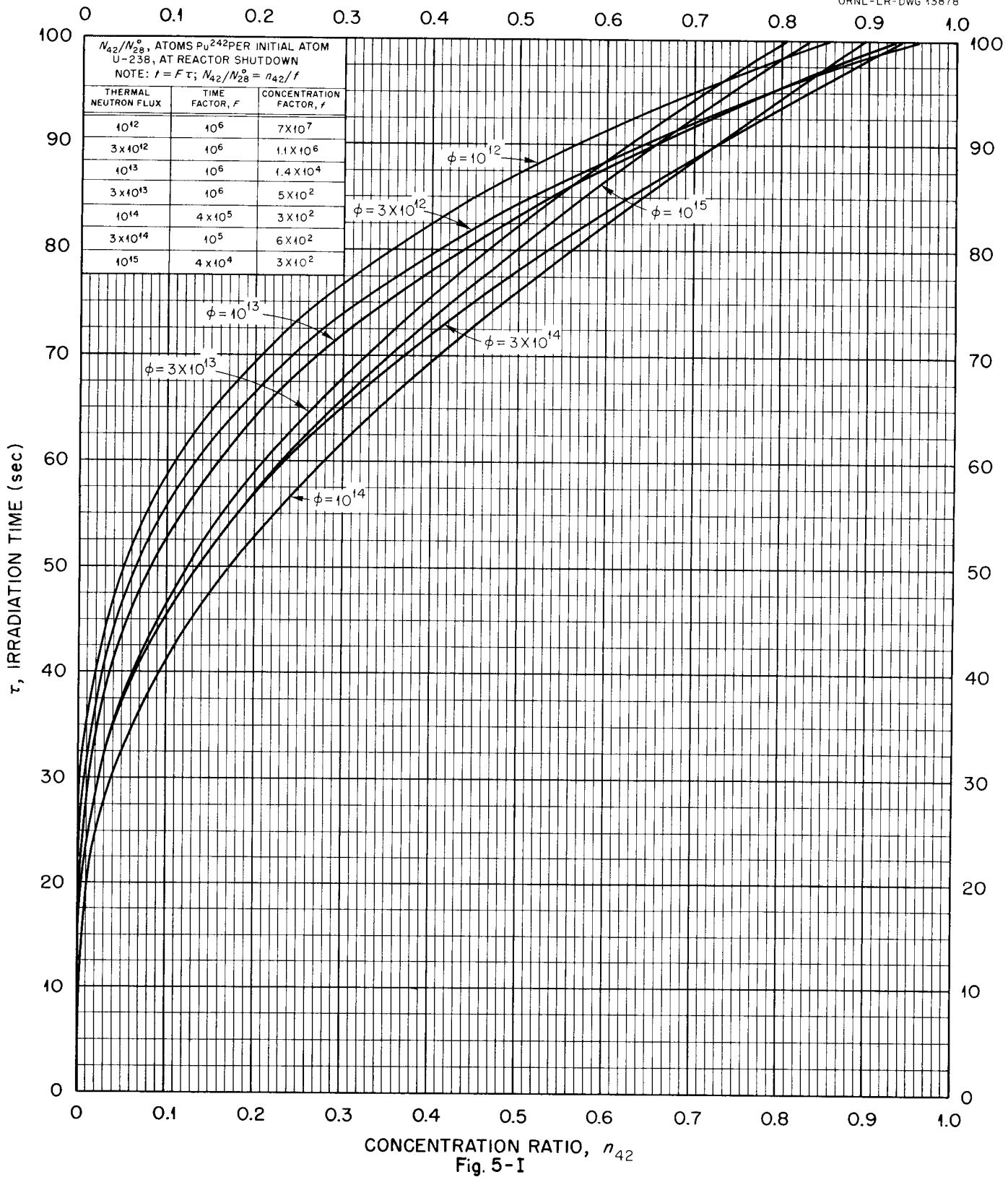
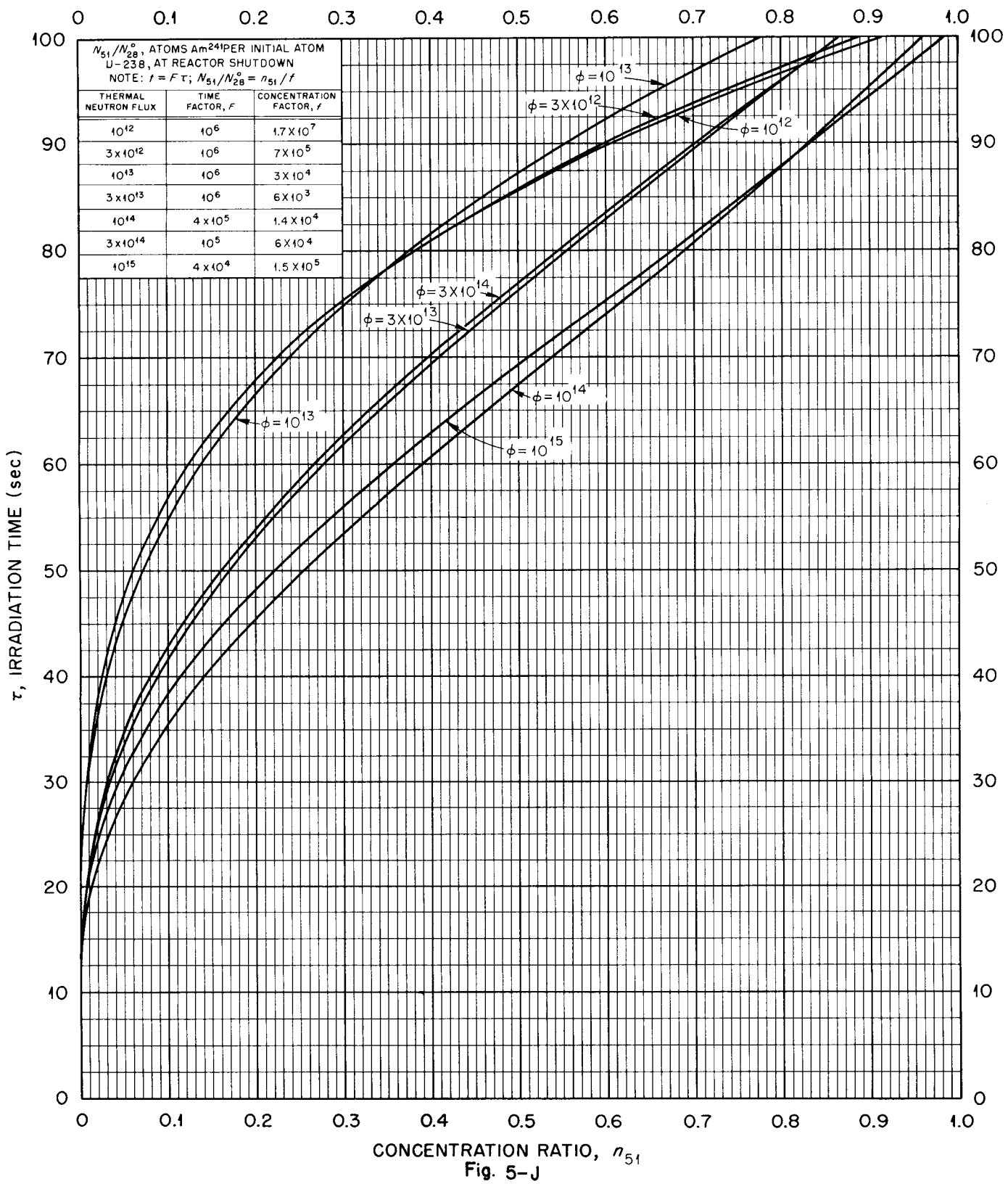
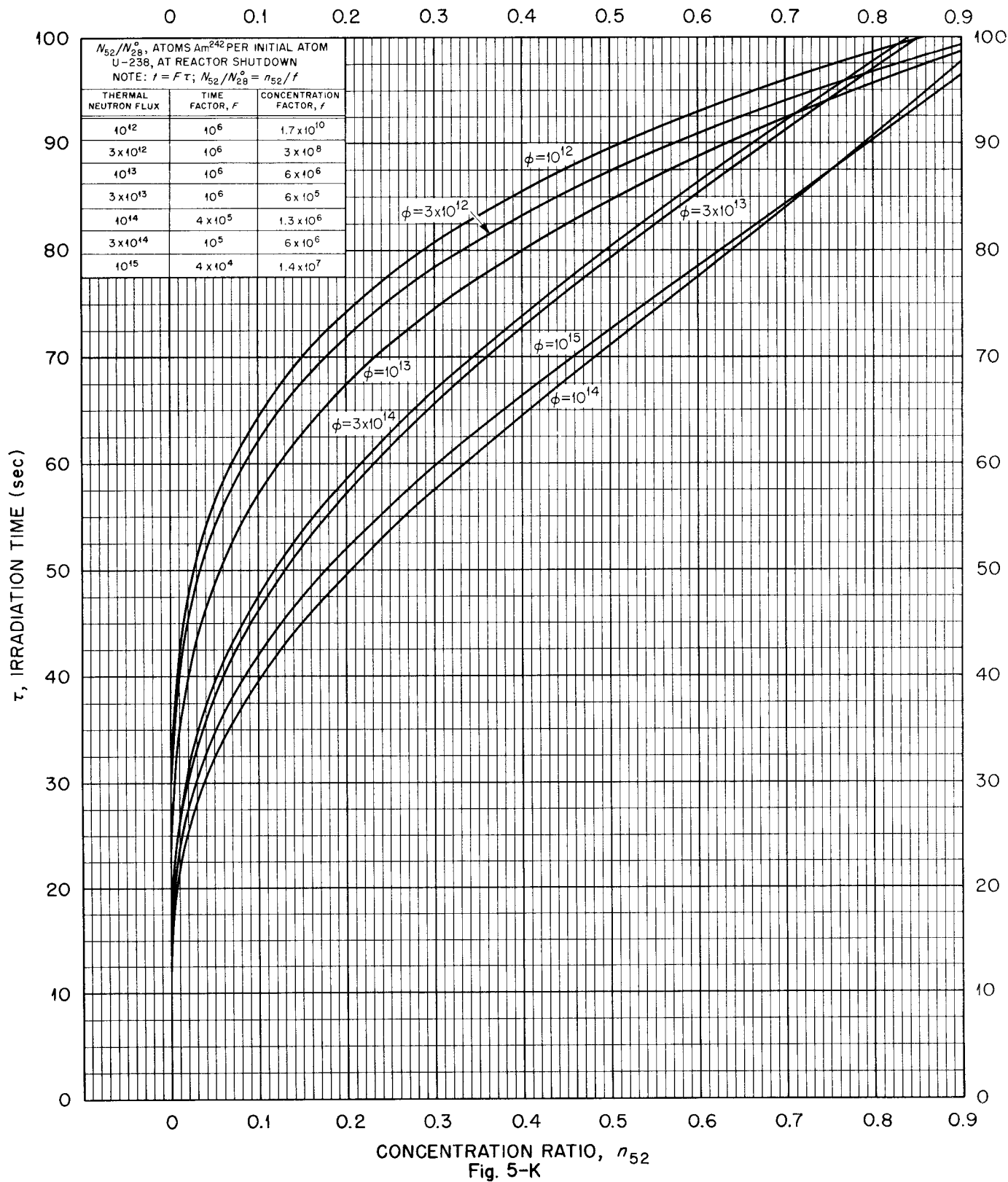
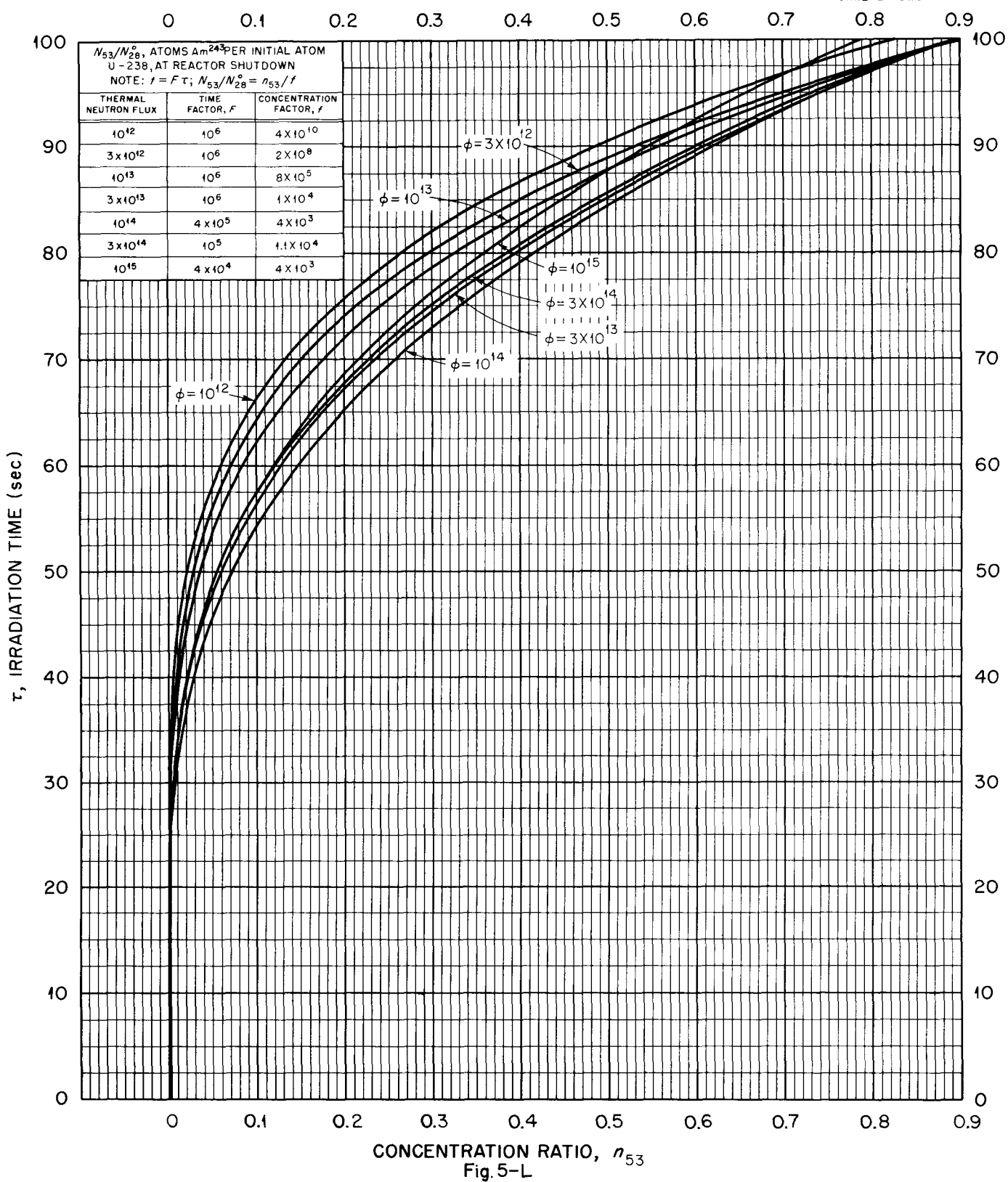


Fig. 5-I







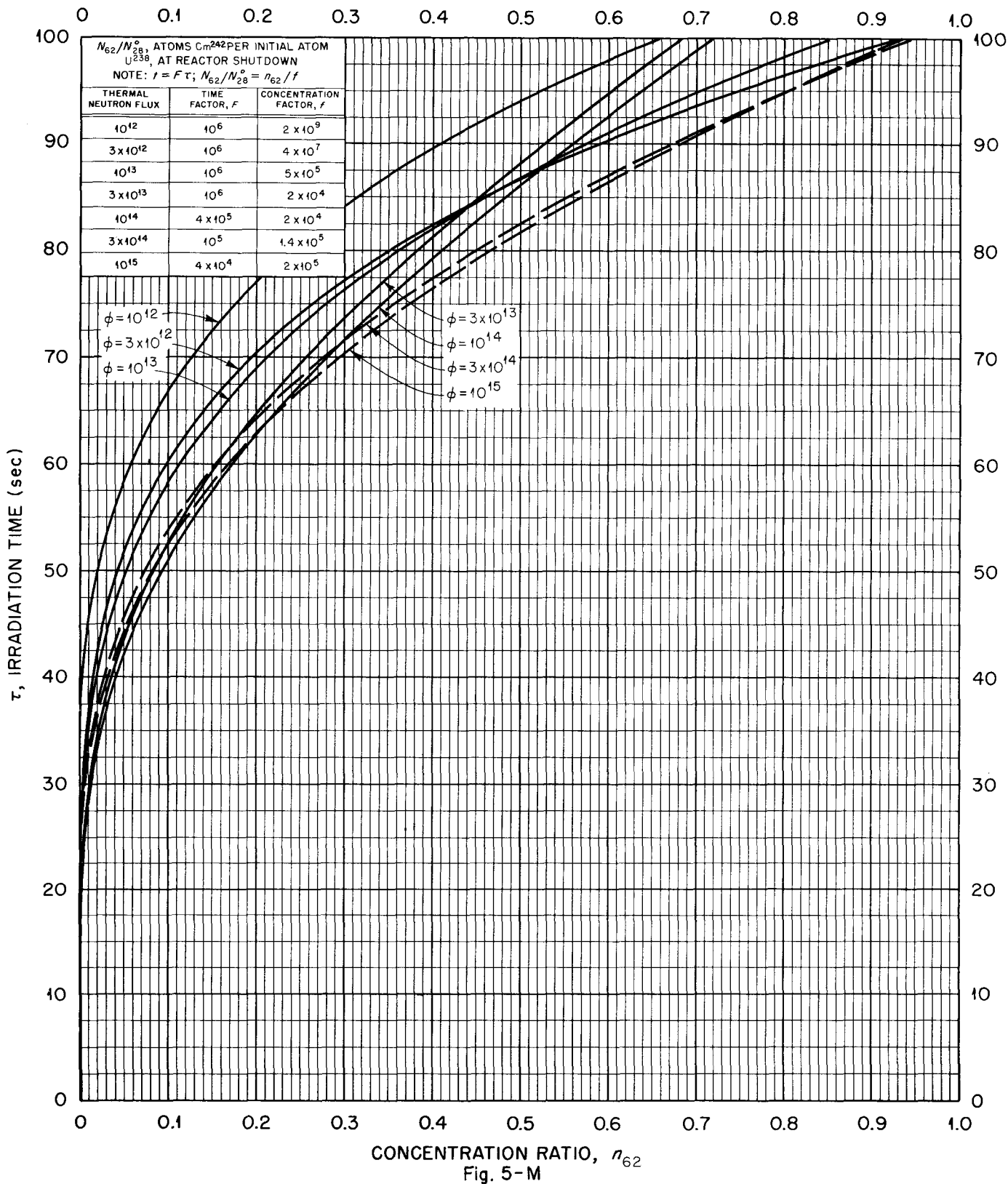


Fig. 5-M

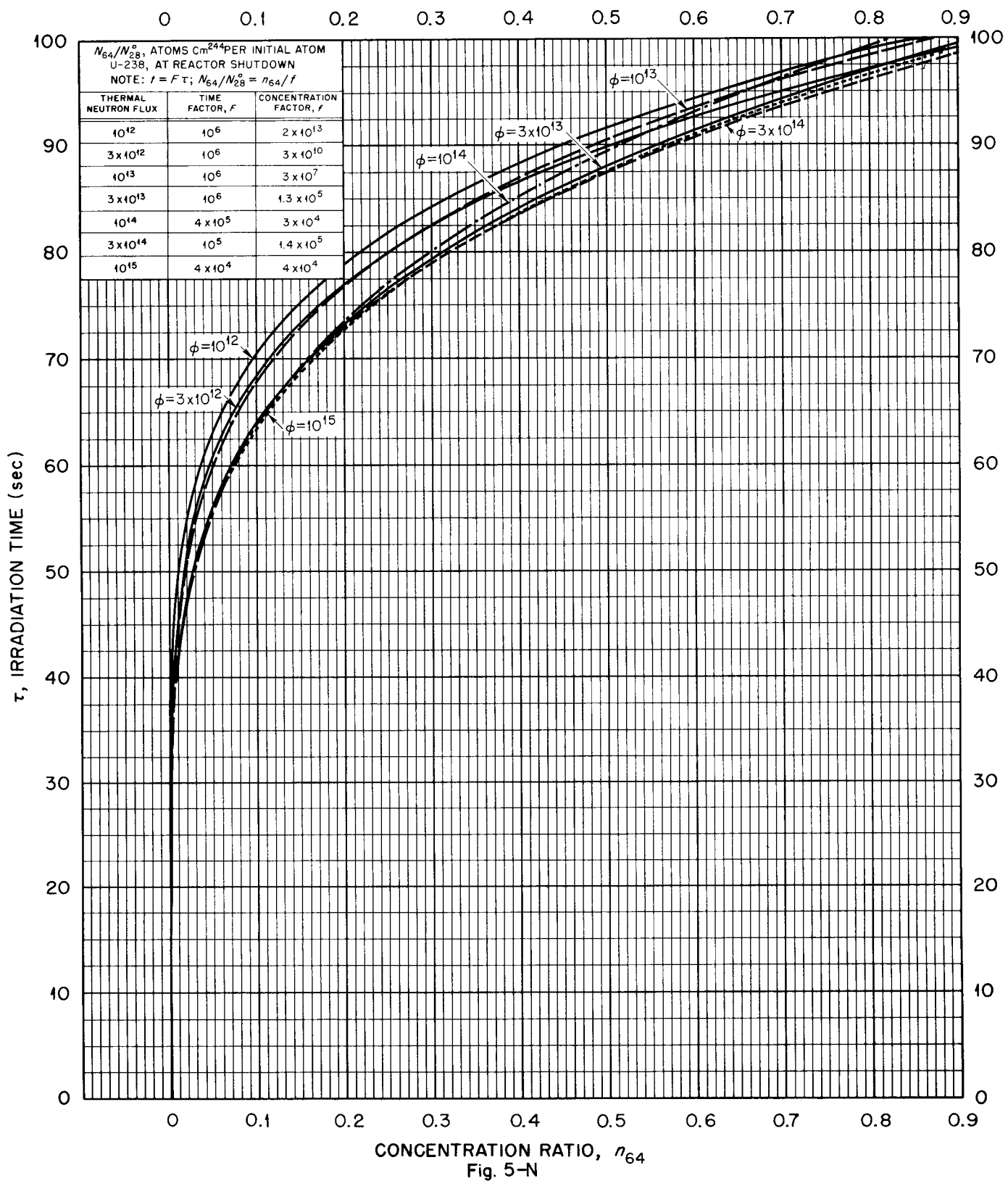


Fig. 5-N